UNIVERSITY OF CALIFORNIA
RIVERSIDE

The Effect of Platinum Surface Structure in the Oxidation of Glycerol

A Thesis submitted in partial satisfaction
of the requirements for the degree of

Master of Science

in

Chemistry

by

Yang Li

December 2014

Thesis Committee:
Dr. Francisco Zaera, Chairperson
Dr. Gregory Beran
Dr. Yadong Yin

The Thesis of Yang Li is approved:

Committee Chairperson

University of California, Riverside

Acknowledgements

I thank Prof. Zaera, for giving me the opportunity to carry out research in the amazing and fascinating area of surface and catalysis, and for his guidance and suggestions throughout the whole period. His keen insight and high standard in science, everlasting passion and self-discipline has been and will always be a role model to me. I also really appreciate his understanding, generosity and support in my difficult times.

I also thank Prof. Beran, Prof. Yin, Prof. Hooley, and Prof. Christopher, for being my committee members and providing valuable comments in SYRE and oral exam.

I really appreciate Dr. Ilkeun Lee for his generous help on every aspect, TEM analysis, guidance in nanoparticle synthesis and IR system, and numerous miscellaneous things in the lab. I also thank Dr. Jibong Joo for his help with the HPLC system. I am grateful to the other colleagues in the lab for their friendship and help, including Xiangdong, Qiang, Huaxing, Shinji, Xin, Menno, Taesung, Yunxi, Karakalos, Aashani, Maryam, Zhihuan, Clinton, Lei, Lanxia, Jie, Xiaoliang, Alex, Carlos, etc.

My deepest gratitude goes to my parents, to whom I owe everything that matters. And I also thank my dearest friends, whose love and understanding has been so important.

This thesis work is funded by National Science Foundation.

Table of Contents

List of Figures

List of Tables

Chapter 1

Introduction

1.1 Overview

One of the major challenges in heterogeneous catalysis today is to design and prepare highly selective catalysts. The difficulty is that highly selective heterogeneous catalysts require solids with large numbers of well-defined active sites designed for the promotion of a particular reaction, and that has been quite difficult to achieve in the past. It is only in recent years, with the advent of self-assembly and other nanotechnologies, that targeting the preparation of solids to promote specific catalytic reactions has become widely possible [1-3]. Those new technologies offer new opportunities in preparing highly selective catalysts by better controlling their structures.

In order to take advantage of the new nanotechnologies in catalysis, a better understanding is needed of how surface structure defines selectivity in specific reactions. In real reaction systems, it is long known that the structure of the catalyst will affect its catalytic behavior for demanding reactions [4-7]. However, they usually require high temperatures and pressures, the original subtle structure of the catalyst may be destroyed. Mild reactions may be able to preserve the structure of the catalyst, but they have been historically considered as structure insensitive [8-10]. However, that conclusion was drawn from studies using ill-defined supported catalysts and newer studies have corroborated that catalysts with well-defined structures may display unique selectivities for particular mild reactions [11-22]. In our lab, it has been demonstrated that, in both real catalyst system [21-22] and surface-science work on single-crystal surface [21; 23-27], the (111) facets of the Pt metal favor the preferential rearrangement of trans-olefins

to their cis counterparts, while its (100) facets (and rougher surfaces) promote the reverse cis-to-trans conversion. These pioneering works indicate that the structure of catalyst may indeed be used to control the selectivity. However, the generality of this behavior still needs to be tested. This is what will be mainly focus on here. In this thesis, proper reaction system and catalysts have been selected to test this generality.

1.2 Glycerol oxidation

The first mild reaction we set out to work with is the oxidation of glycerol. It is a reaction of essential importance both in the industry and to the fundamental research of structure-selectivity relationship in heterogeneous catalysis. In this section, the reason for selecting this system and its potentials will be stated.

1.2.1 Glycerol oxidation in the biomass industry

Petroleum has been the major source of fuel and chemicals for decades. Ever since the energy crisis in the last 70s, the conflict between the non-renewability of fossil fuels and rapid development of the society has been widely recognized. The energy crisis as well as the eco-crisis has driven the search for renewable sources of transportation fuel and fine chemicals. Biomass, with its abundance and; green and renewable nature, has become the most promising and widely accepted candidate to replace petroleum and provide fuel and chemicals to the human endeavor. Glycerol is of great importance in the biomass industry, as it is the major byproduct of biodiesel production and an important platform molecule

in biomass conversion. The oxidation of glycerol is one of the major routes to convert and utilize glycerol.

Glycerol is the major byproduct of biodiesel production. Biodiesel is renewable and can directly replace fossil fuels, and therefore has been considered the ideal solution for the global energy crisis. The main composition of biodiesel is fatty acid esters. It can be synthesized from cheap raw materials such as oil-bearing crops, used cooking oil, animal fat and organic waste from industrial manufacturing through an ester exchange reaction. Compared to traditional diesel, biodiesel has the following advantages [28]: (1) it is more environmental friendly due to its low sulfur content, its lack of aromatic hydrocarbons, its reduced smoke generation, and its high bio-degradability; (2) it displays excellent low temperature start; (3) it has excellent lubricating properties; (4) it is safer due to its high flash point; (5) it shows better combustion performance; (6) it is renewable; (7) it does not require any engine modifications; and (8) it can alleviate the greenhouse effect.

According to the literature, on average, 1 kg of glycerol is produced for every 9 kg of biodiesel [29]. This has caused a supply exceeding demand in the glycerol market, and traditional glycerol production units have been closing down. This indicates that pursuing new applications for glycerol, increasing its additional value, could significantly reduce its cost and promote biodiesel production.

In addition, glycerol is also an important platform molecule in biomass conversion. Biomass-derived polyols, including glycerol, sorbitol, xylitol, mannitol, maltose, and others, are abundant in nature, and have traditionally been used in food, cosmetic and medical industry. In recent years, people have started to focus on converting biomass polyols to high-valued fine chemicals [30-32]. Their clean and renewable properties and the fact that they exhibit multifunctional groups make them promising substitutes for the petrochemical industry. Glycerol, together with some other polyols, can be used as platform molecules to convert to other chemicals or biofuels [30; 33-34]: glycerol can be selectively oxidized to glyceraldehyde, dihydroxyacetone, lactic acid and glyceric acid [35], dehydrated to form acraldehyde [36-37] and hydroxyacetone [38], selectively hydrogenated to form 1,2-propylene glycol [29; 39-43] and 1,3-propylene glycol [44-45], or carbonylated to form glycerol carbonate [46-48].

Although people have started to explore the conversion of polyols, their selective catalytic conversion has not been achieved yet, and the reaction mechanisms involved remain unclear. Given that glycerol is the most simple-structured molecule among those multi-hydroxyl group compounds, its conversion is also of essential importance to study other biomass-derived polyols.

1.2.2 Structure sensitivity of glycerol oxidation

As indicated above, it is our premise that the catalytic conversion of glycerol may be structure sensitive. In order to preserve the fine structure of well-defined catalyst during

the reactions, the reaction conditions used have to be relatively mild. Most of the oxidation processes are exothermic and are carried out under harsh conditions (higher temperatures and high pressures), but glycerol oxidation can be carried out under relatively mild conditions, as the glycerol molecule already have three hydroxyl groups. It has already shown in many reports that glycerol can be oxidized to a considerable degree under atmospheric pressure and below 100℃ [49-50; 54-55; 57-58].

Some recent studies have indicated that this reaction might be surface structure sensitive [35; 49-51]. One particularly relevant work by Lin et al. [49] shows that carbon nanotube-supported Pt particles with rough edges show high selectivity toward glyceraldehyde, while regular active carbon supported Pt catalyst promotes the formation of dihydroxyacetone and glyceric acid instead. Another report by Liang et al. [50] indicates that the selectivity of Pt/C catalysts toward the oxidation of glycerol to glyceric acid increases with the size of the Pt nanoparticles.

When this reaction is catalyzed by other metals, it also shows some structure sensitivity. In the work of Dimitratos et al. [51], a size effect was observed with Au, Pd and Au-Pd catalysts: as the size of the metal particles increases, the activity of the catalysts decreases while the selectivity toward glyceric acid increases. Moreover, at higher temperatures, larger particles still favor glyceric acid production while smaller particles further oxidize glycerol to tartronic acid. In the work of Ketchie et al. [35], Au catalysts with different

particle sizes have been compared, and similar results were observed, namely, larger Au particles show less reactivity but higher selectivity toward glyceric acid.

However, the above-mentioned studies have been far from thorough in terms of proving the structure-selectivity relationship or revealing the mechanism of this relationship in this system. In the work by Lin et al. [49], the result of carbon nanotube-supported Pt catalysts (Pt/CNTs) is compared with an active carbon supported Pt (Pt/C) sample from another report [50], not from their own lab. Also, no information was provided about the kinetics of conversion of the glycerol or the reaction time, both of which may affect the selectivity of the reaction. Moreover, the given reaction conditions are very different from those they use for the comparison: the glycerol concentration is 2wt% and 10wt% respectively, the O_2 flow rate is 65 mL/min, compared to 150 mL/min, and there is also a large difference in the amount of catalyst used, 25 mg of 0.77 wt% Pt/CNTs versus 500 mg of 5 wt% Pt/C. All these changes of parameter could have large effects on the results. The major selectivity difference they listed is between glyceraldehyde and glyceric acid, while the conversion from glyceraldehyde to glyceric acid depends quite largely on time and O_2 flow rate. Furthermore, there is not sufficient structure information about the Pt/C catalyst to compare it with the Pt/CNTs catalyst. It should also be noticed that completely different preparation methods were used for the two kinds of catalysts, and that the leftover protecting agent and inorganic ions used in the synthesis on the catalyst surface may have a potential large effect on the catalysis too. Without excluding the effects of other experimental parameters and showing no direct evidence to relate Pt structure with

selectivity, there is no enough evidence to attribute the difference in the selectivity of glycerol oxidation to the differences in Pt surface structure. The conclusion that Pt with stepped surface induces selective oxidation, effectively ceasing at the stage of glyceraldehyde, may not necessarily be right. Similar problems can be identified with the other reports. The characteristics of the metal catalysts in those comparisons are usually not well controlled. The particle size is only one of many differences among the catalysts used, and even there the catalysts usually have quite broad size distributions too. The reactions that were reported to show differences in selectivity were all carried out under different glycerol conversions, while for the catalysts showing similar conversions, the selectivities were quite close.

Although the conclusions of these works remain questionable, they reveal an interesting and complex picture for glycerol oxidation. A complete review of glycerol oxidation studies in the literature is therefore also necessary to further evaluate the possibility of a structure sensitivity for this reaction. To the best of our knowledge, the first paper on metal catalyzed oxidation of glycerol dates back to 1983 [52], and so far there are around one hundred papers about this reaction under conditions of heterogeneous catalysis, enzymatic catalysis, homogeneous catalysis, and electro-catalysis, among which heterogeneous catalysis is the predominant method used. Among these papers, two interesting major discoveries can be identified: (1) When Bi is added to Pt catalysts, the selectivity is reversed from favoring primary carbons to favoring secondary carbons, a change that results in a large increase in dihydroxyacetone selectivity [53-59]; and (2)

When Au is mixed with Pt and Pd, the bimetallic catalysts (not necessarily alloys) show better performance than the pure metals, and very high selectivity toward glyceric acid [51; 61-65]. The case of Pt and Bi is particularly interesting, as Bi by itself has no activity under those conditions. In the work of Mallat et al. [60], they use XPS to show that Bi atoms are on the surface of Pt but do not change the electronic state of that metal. Kimura et al. [54] speculate that Bi may change the adsorption state of glycerol on Pt to lead to selectivity toward oxidation of secondary carbons. These evidence from literature show enough potential that glycerol oxidation could be structure sensitive, and also provide some insights on the possible mechanism.

Compared to other metals used for this reaction, such as Au, Pd, Ru or bimetallic solids, Pt is a relatively mild catalyst for this reaction. Further oxidation leading to the break-down of carbon-carbon bonds is rarely observed on Pt catalysts. For an already complex reaction system as glycerol oxidation, relative control of the oxidation process with less elementary steps involved makes it relatively easier to eliminate disturbing factors and to identify the real influencing factors controlling selectivity, therefore helping to obtain a clearer picture and a deeper understanding of the catalyzed oxidation mechanism. Moreover, although Pt is a relatively mild catalyst, it still can catalyze the oxidation of glycerol under neutral, and even acidic, environment, unlike Au, which only works in basic solutions. This also makes a big difference for this system. The first step in the oxidation of glycerol may yield two products, glyceraldehyde and dihydroxyacetone, depending on whether primary or secondary carbons are oxidized first and under basic

conditions, these two products may interconvert into each other in solution without the help from the catalyst [32]. Luckily, this does not happen in neutral or acidic solutions. Using Pt also helps in the observation of the essential selectivity of the metal catalyst without the interference from further conversions happening outside the interface.

In terms of preparing well defined catalysts, the synthesis of Pt nanoparticles has been widely explored, and recipes of Pt nanoparticles with various shapes such as tetrahedron, cube, cuboctahedron, tetrapod, nanodendrite, nanowire, nanowire network, tetrahexahedron are available from the literature [66]. It should be possible to take advantage of these reported nanotechnologies to study the structure-selectivity relationship in catalysis discussed above. We expect that different Pt surface structures to favor different adsorption states of the reactant and therefore to dictate the selectivity of these oxidation reactions.

1.3 Thesis objective and organization

The hypothesis of this research is that the surface structure of solid catalysts may affect the selectivity of many mild reactions. Therefore, the objective of this research is to explore the generality of this hypothesis by using well-defined supported metal catalysts. The steps followed toward this goal can be divided into as follows:

1. Synthesize well-defined supported metal catalysts of various uniform crystal shapes and narrow size distributions.

2. Test the metal catalysts under the mild reactions that potentially lead to the expected surface structure sensitive.
3. Study the structure sensitivity of these reactions in detail by using surface-science techniques and kinetic studies of the reaction.

In chapter 3, the results from a general study on glycerol oxidation kinetics are reported in order to gain a basic knowledge of this reaction, including the appropriate reaction condition, the identification of the major products, and establish how reaction conditions such as temperature, O_2 flow rate, reaction time and catalyst pretreatment may affect activity and selectivity, and lay out the foundations for studying the structure-selectivity relationship discussed in the following chapters.

Chapter 4 focuses on the relationship between the catalyst structure and the selectivity of the glycerol oxidation. Pt catalysts with various particle sizes and shapes were for the glycerol oxidation reaction under appropriate conditions. Obvious differences and trends in product selectivity were observed and further studied by kinetic experiments and catalyst characterizations.

In chapter 5, a summary, our conclusions, and our suggestions for future work are provided.

1.4 References

[1] F. Zaera, *J. Phys. Chem. Lett.* **2010**, 1, 621-627.

[2] C. Burda, X. Chen, R. Narayanan, M. A. El-Sayed, *Chem. Rev.* **2005**, 105, 1025-1102.

[3] G. Somorjai, C. Kliewer, *React. Kinet. Catal. Lett.* **2009**, 96, 191-208.

[4] M. Boudart, *Adv. Catal.* **1969**, 20, 153-166.

[5] G. C. Bond, *Metal-Catalysed Reactions of Hydrocarbons*, Springer, New York, **2005**.

[6] F. Zaera, A. J. Gellman, G. A. Somorjai, *Acc. Chem. Res.* **1986**, 19, 24-31.

[7] Z. Ma, F. Zaera, *Surf. Sci. Rep.* **2006**, 61, 229-281.

[8] B. C. Gates, J. R. Katzer, G. C. A. Schuit, *Chemistry of Catalytic Processes*, McGraw-Hill, New York, **1979**.

[9] F. M. Dautzenberg, J. C. Platteeuw, *J. Catal.* **1972**, 24, 364-365.

[10] H. Yoshitake, Y. Iwasawa, *J. Phys. Chem.* **1992**, 96, 1329-1334.

[11] K. M. Bratlie, H. Lee, K. Komvopoulos, P. Yang, G. A. Somorjai, *Nano Lett.* **2007**, 7, 3097-3101.

[12] C-K Tsung, J. N. Kuhn, W. Huang, C. Aliaga, L-I Hung, G. A. Somorjai, P. Yang, *J. Am. Chem. Soc.* **2009**, 131, 5816-5822.

[13] S. Alayoglu, C. Aliaga, C. Sprung, G. A. Somorjai, *Catal. Lett.* **2011**, 141, 914-924.

[14] R. M. Rioux, B. B. Hsu, M. E. Grass, H. Song, G. A. Somorjai, *Catal. Lett.* **2008**, 126, 10-19.

[15] M. E. Grass, R. M. Rioux, G. A. Somorjai, *Catal. Lett.* **2009**, 128, 1-8.

[16] C. J. Kliewer, G. A. Somorjai, *Catal. Lett.* **2010**, 137, 118-122.

[17] V. V. Pushkarev, K. An, S. Alayoglu, S. K. Beaumont, G. A. Somorjai, *J. Catal.* **2012**, 292, 64-72.

[18] V. V. Pushkarev, N. Musselwhite, K. An, S. Alayoglu, G. A. Somorjai, *Nano Lett*. **2012**, 12, 5196-5201.

[19] V. D. Michalak, J. M. Krier, K. Komvopoulos, G. A. Somorjai, *J . Phys. Chem. C* **2013**, 117, 1809-1817.

[20] I. Lee, R. Morales, M. A. Albiter, F. Zaera, *Proc. Natl. Acad. Sci.* **2008**, 105, 15241-15246.

[21] I. Lee, F. Delbecq, R. Morales, M. A. Albiter, F. Zaera, *Nat. Mater.* **2009**, 8, 132-138.

[22] I. Lee, F. Zaera, *J. Catal.* **2010**, 269, 359-366.

[23] I. Lee, F. Zaera, *J. Am. Chem. Soc.* **2005**, 127, 12174-12175.

[24] I. Lee, F. Zaera, *J. Phys. Chem. B* **2005**, 109, 2745-2753.

[25] I. Lee, F. Zaera, *J. Phys. Chem. C* **2007**, 111, 10062-10072.

[26] I. Lee, M. K. Nguyen, T. H. Morton, F. Zaera, *J. Phys. Chem. C* **2008**, 112, 14117-14123.

[27] I. Lee, J. Hong, F. Zaera, *J. Phys. Chem. C* **2011**, 115, 982-989.

[28] J. Hill, E. Nelson, D. Tilman, S. Polasky, D. Tiffany, *Proc. Natl. Acad. Sci.* **2006**, 103, 11206-11210.

[29] M. A. Dasari, P. P. Kiatsimkul, W. R. Sutterlin, G. J. Suppes, *Appl. Catal. A* **2005**, 281, 225-231

[30] A. Corma, S. Iborra, A. Velty, *Chem. Rev.* **2007**, 107, 2411-2502.

[31] D. A. Simonetti, J. A. Dumesic, *Catal. Rev. Sci. Eng.* **2009**, 51, 441-484

[32] Y. Shen, S. Zhang, H. Li, Y. Ren, H. Liu, *Chem. Eur. J.* **2010**, 16, 7368-7371.

[33] E. L. Kunkes, D. A. Simonetti, R. M. West, J. C. Serrano-Ruiz, C. A. Gartner, J. A. Dumesic, *Science* **2008**, 322, 417-421

[34] S. Fernando, S. Adhikari, C. Chandrapal, N. Murali, *Energy & Fuels* **2006**, 20, 1727-1737

[35] W. C. Ketchie, Y-L, Fang, M. S. Wong, M. Murayama, R. J. Davis, *J. Catal.* **2007**, 250, 94-101.

[36] S. Chai, H. Wang, Y. Liang, B. Xu, *Green Chem.* **2007**, 9, 1130-1136

[37] F. Wang, J. L. Dubois, W. Ueda, *J. Catal.* **2009**, 268, 260-267.

[38] S. Sato, M. Akiyama, R. Takahashi, T. Hara, K. Inui, M. Yokota, *Appl. Catal. A* **2008**, 347, 186-191

[39] T. Miyazawa, Y. Kusunoki, K. Kunimori, K. Tomishige, *J. Catal*. **2006**, 240, 213-221

[40] S. Wang, H. Liu, *Catal. Lett*. **2007**, 117, 62-67.

[41] M. Akiyama, S. Sato, R. Takahashi, K. Inui, M. Yokota, *Appl. Catal. A* **2009**, 371, 60-66

[42] X. Guo, Y. Li, R. Shi, Q. Liu, E. Zhan, W. Shen, *Appl. Catal. A* **2009**, 371, 108-113

[43] W. Yu, J. Xu, H. Ma, C. Chen, J. Zhao, H. Miao, Q. Song, *Catal. Commun*. **2010**, 11, 493-497

[44] T. Kurosaka, H. Maruyama, I. Naribayashi, Y. Sasaki, *Catal. Commun.* **2008**, 9, 1360-1363

[45] L. Huang, Y. Zhu, H. Zheng, G. Ding, Y. Li, *Catal. Lett*. **2009**, 131, 312-320

[46] C-H. Zhou, J. N. Beltramini, Y-X. Fan, G. Q. Lu, *Chem. Soc. Rev.* **2008**, 37, 527-549.

[47] M. Pagliaro, R. Ciriminna, H. Kimura, M. Rossi, C. D. Pina, Angew. *Chem. Int. Ed.* **2007**, 46, 4434-4440.

[48] Y. Zheng, X. Chen, Y. Shen, *Chem. Rev*. **2008**, 108, 5253-5277

[49] Z. Lin, H. Chu, Y. Shen, L. Wei, H. Liu, Y. Li, *Chem. Commun.* **2009**, 7167-7169.

[50] D. Liang, J. Gao, J. Wang, P. Chen, Z. Hou, X. Zheng, *Catal. Commun.* **2009**, 10, 1586-1590.

[51] N. Dimitratos, J. A. Lopez-Sanchez, D. Lennon, F. Porta, L. Prati, A. Villa, *Catal. Lett.* **2006**, 108, 147-153.

[52] G. Horanyi, E.M. Rizmayer, *Acta Chemica Scandinavica B* **1983**, 37,451-457.

[53] H. Kimura, *Appl. Catal. A* **1993**, 105, 147-158.

[54] H. Kimura, K. Tsuto, *Appl. Catal. A* **1993**, 96, 217-228.

[55] R. Garcia, M. Besson, P. Gallezot, *Appl. Catal. A* **1995**, 127, 165-176.

[56] W. Hu, D. Knight, B. Lowry, A. Varma, *Ind. Eng. Chem. Res.* **2010**, 49, 10876-10882.

[57] N. Wörz, A. Brandner, P. Claus, *J. Phys. Chem. C* **2010**, 114, 1164-1172.

[58] D. Liang, S. Cui, J. Gao, J. Wang, P. Chen, Z. Hou, Chin. *J. Catal.* **2011**, 32, 1831-1837.

[59] M. Simões, S. Baranton, C. Coutanceau, *Appl. Catal. B* **2011**, 110, 40-49.

[60] T. Mallat, Z. Bodnar, P. Hug, A. Baiker, *J. Catal.* **1995**, 153, 131-143.

[61] C. L. Bianchi, P. Canton, N. Dimitratos, F. Porta, L. Prati, *Catal. Today* **2005**, 102-103, 203-212.

[62] A. Villa, G. M. Veith, L. Prati, *Angew. Chem. Int. Ed.* **2010**, 122, 4601-4604.

[63] D. I. Enache, J. K. Edwards, P. Landon, B. Solsona-Espriu, A. F. Carley, A. A. Herzing, M. Watanabe, C. J. Kiely, D. W. Knight, G. J. Hutchings, *Science* **2006**, 311, 362-365.

[64] N. Dimitratos, J. A. Lopez-Sanchez, J. M. Anthonykutty, G. Brett, A. F. Carley, R. C. Tiruvalam, A. A. Herzing, C. J. Kiely, D. W. Knight, G. J. Hutchings, *Phys. Chem. Chem. Phys*. **2009**, 11, 4952-4961.

[65] G. L. Brett, Q. He, C. Hammond, P. J. Miedziak, N. Dimitratos, M. Sankar, A. A. Herzing, M. Conte, J. A. Lopez-Sanchez, C. J. Kiely, D. W. Knight, S. H. Taylor, G. J. Hutchings, *Angew. Chem. Int. Ed.* **2011**, 50, 1-4.

[66] Y. Xia, Y. Xiong, B. Lim, S. E. Skrabalak, *Angew. Chem. Int. Ed.* **2009**, 48, 60-103.

Chapter 2

Experimental Details

The experimental details of the work in this thesis are given below. In the following chapters only the key conditions for each set of experiments are indicated; the detailed procedures are not described again. It is important to note that for both the catalyst synthesis and the catalytic reaction kinetic studies, due to their complex and sensitive nature, the experimental details are likely to affect the outcome and the reproducibility of the result.

2.1 Chemical reagents

Catalyst synthesis: Dihydrogen hexachloroplatinate (IV) hexahydrate ($H_2PtCl_6 \cdot 6H_2O$, 99.9%) from Alfa Aesar, $Pt(NH_3)_4Cl_2 \cdot xH_2O$ (98%) from Sigma-Aldrich, K_2PtCl_4 (98%) from Sigma-Aldrich, silica (fumed powder, S5505) from Sigma-Aldrich, AEROSIL fumed silica (A200) from Evonik, polyvinylpyrrolidone (PVP, MW 360,000), sodium polyacrylate (SPA, MW 2,100). Glycerol Oxidation: Glycerol (≥99.5%) from Sigma-Aldrich. Product Analysis: Acetonitrile (HPLC grade) from Fisher Scientific, Phosphoric Acid (85 wt%), NaOH (pellets, 98%), methanol (HPLC Grade, 99.8+%) from Alfa Aesar, 1,3-Dihydroxyacetone Dimer (>96.0%) from TCI, DL-glyceraldehyde Dimer (≥97.0%) from Sigma-Aldrich, DL-glyceric acid (20% in water, ca. 2mol/L) from TCI, formic acid (97%) from Alfa Aesar, glycolic acid (98%) from Alfa Aesar, lactic acid (1.0 N standardized solution) from Alfa Aesar, Tartronic acid (98%) from Alfa Aesar, pyruvic acid (98%) from Alfa Aesar, sodium mesoxalate monohydrate (≥98.0%) from Sigma-Aldrich.

2.2 Catalyst preparation

Most of the Pt/SiO_2 catalysts synthesized in this thesis include regular Pt/SiO_2, tetrahedral Pt/SiO_2 or cuboctahedral Pt/SiO_2. Their preparation methods are described below.

2.2.1 Regular Pt/SiO2

Reference to regular Pt/SiO_2 here means to the catalysts for which, during the synthesis, the shape of Pt particle is not specifically designed. In this thesis, an impregnation method was used to synthesize the regular Pt/SiO_2. As various precursors, solvents and treatments were used, these different conditions will be marked in the following chapters when regular Pt/SiO_2 is used. The Pt precursor was dissolved in the impregnation solvent to form a homogeneous solution. The SiO_2 powder used as the support was also dissolved in the same kind of solvent, and ultra-sonicated to form a homogeneous-looking slurry. In some cases, the pH values of the solutions were adjusted by adding $NH_4{\cdot}OH$ or HCl to increase the strength of the interaction between the Pt precursor ions and surface of the silica. The two were then mixed, sonicated, and stirred overnight. The mixture was sonicated again the next day, and that was followed by rotary evaporation. The catalyst was usually dried under 110℃ for 30 min in an oven.

2.2.2 Shape controlled Pt/SiO_2

Various methods for synthesizing Pt nanoparticles with well-defined shapes have been reported in literature [1]. After several trials, we focused on two of those relatively stable

and reproducible synthetic methods. The synthesis was based on the recipes previously used in our lab [2-3], which were initially taken from the recipe reported by El-sayed et al. [4].

Tetrahedral Pt nanoparticles were synthesized by reducing a K_2PtCl_4 precursor under the protection of PVP (polyvinylpyrrolidone). 15 mL of distilled H_2O, 1.0 mL of a PVP solution (10^{-6} M aq, MW 360,000), and 0.2-0.3 g (accurately measured by electronic scale) of a K_2PtCl_4 solution (0.01M aq) were mixed in a 11 drams vial and capped and stirred for 10 min. Then, He gas was bubbled into the solution for 10 min while stirring, and H_2 was bubbled into the solution at the rate of 1-2 bubble/second for 2 min. Finally, the solution was sealed and stored in the dark for at least 12 hours before use.

Cuboctahedral Pt nanoparticles were synthesized by reducing the K_2PtCl_4 precursor under the protection of SPA (sodium polyacrylate). 15 mL of distilled H_2O, 0.2 mL of a SPA solution (0.01 M aq, MW 2,100), and 0.2-0.8 g (accurately measured by electronic scale) of a K_2PtCl_4 solution (0.01M aq) were mixed in a 11 drams vial. The rest of the procedure was the same as that use for tetrahedral Pt nanoparticles.

The as-synthesized colloidal particles were loaded onto the silica supports to form powder Pt/SiO_2 catalysts. Using an impregnation method, these nanoparticles were successfully dispersed onto the surface of SiO_2 support. A designated amount of the SiO_2 support was added to the vial containing the colloidal solution. The mixture was stirred

overnight and sonicated for 30 min, followed by either vacuum filtration or rotary evaporation. The well-shaped catalysts were also be dried under 110℃ for 30 min in an oven.

2.2.3 Calcination and pretreatment

In most of the synthesis, calcination was used to fix the Pt particle onto the SiO_2 support and stabilize the catalyst structure. Calcination was either carried out in a muffle furnace or in a gas-flow furnace. The gas atmosphere in the muffle furnace was air. There was very limited air flow in the muffle furnace, while in the gas-flow furnace, the flow-rate could be adjusted and the atmosphere could be chosen from among H_2, O_2 and He gases. The calcination conditions used are indicated in each case in the following chapters.

For Pt catalysts synthesized from colloidal Pt nanoparticles with protecting polymers, an O_2/H_2 treatment was applied in some cases to remove the polymer in some cases. The catalysts were placed in the air-flow furnace and heated to the designated temperature under O_2 flow, and kept under those conditions for half an hour. The catalysts were then cooled down, the O_2 atmosphere replaced by He, and then by H_2, and the samples were heated again up to the designated temperature. This procedure was counted as one cycle of O_2/H_2 treatment. The temperature and time of the treatment will be indicated as the different experiments are reported. The gas flow rate used was 20-30 mL/min if nodifferent condition is mentioned.

2.3 Catalyst characterization

2.3.1 Transmission electron microscopy (TEM)

TEM characterization was carried out by Dr. Ilkeun Lee using a PHILIPS TECNAI 12 Transmission Electron Microscope (120 kV accelerating voltage). The TEM grids used were Formvar/Carbon Film 400 mesh.

Colloidal nanoparticle solutions were directly used to prepare the TEM samples. For the powder samples, a small amount of the solid was dispersed in distilled water by ultra-sonication, and one drop of the sample solution or suspension was deposited onto the TEM grid and air-dried under room temperature before use.

2.3.2 CO-IR titration

The Fourier-transform infrared (FTIR) instrument used for this system is a Bruker Vector 22. The sample cell is tightly closed with NaCl windows on both sides, and equipped with a thermocouple close to the sample stand used for temperature monitoring. The IR cell is equipped with a heating mantle, a cooling water line and a vacuum line around the cell. By using a combination of liquid nitrogen, the vacuum line, and the heating mantle, the temperature of the cell can be adjusted from -160 ℃ to 600 ℃.

The solid catalysts were grinded in an agate mortar, and pressed into a pellet. Usually 10 mg of the sample was used to prepare one pellet. The sample was placed in the press module, and pressed into a translucent pellet.

The sample pellet was then placed in the IR cell in a standing up position. The cell position was adjusted to get the most coverage of the sample by the IR beam while also getting the maximized absorbance signal. The sample was then pretreated in situ when necessary, a procedure that included drying, calcination under O_2, H_2, and pumping under vacuum. For the CO adsorption experiment, the cell was evacuated at the designated temperature, and the background spectra were taken. The CO was introduced into the cell and kept for a designated amount of time. Then the cell was pumped again for at least 15 min and the sample spectra taken afterwards. The sample used for the CO-IR experiment was never used in the reaction kinetics studies again. The OPUS software provided with the FTIR instrument was used for data processing. Detailed information of in situ treatment and the CO pressures and temperatures used are indicated in the following chapters.

2.4 Glycerol oxidation reaction kinetic measurements

Glycerol oxidation was carried out under ambient pressure. A scheme of the reaction system is shown in Figure 2.1. A 50 mL four-neck round-bottomed flask was used as the main reactor. The center neck was connected to an Allihn condenser which was connected to the ventilator. All the other necks were closed by rubber stoppers. Pure O_2 gas was bubbled into the mixture through thin plastic tubes inserted into both left and right necks. The O_2 amount was adjusted by a flowmeter. A thermocouple was inserted into the mixture through the front neck and connected to a temperature controller to set and keep the reaction temperature. The flask was heated by using a hemispherical heating

mantle controlled by the temperature controller and a voltage variac. A magnetic bar was used for stirring of the mixture. The detailed parameters such as the temperature, the O_2 flow rate, the glycerol concentration, and the type and amount of catalyst used was varied in the different reaction kinetic studies.

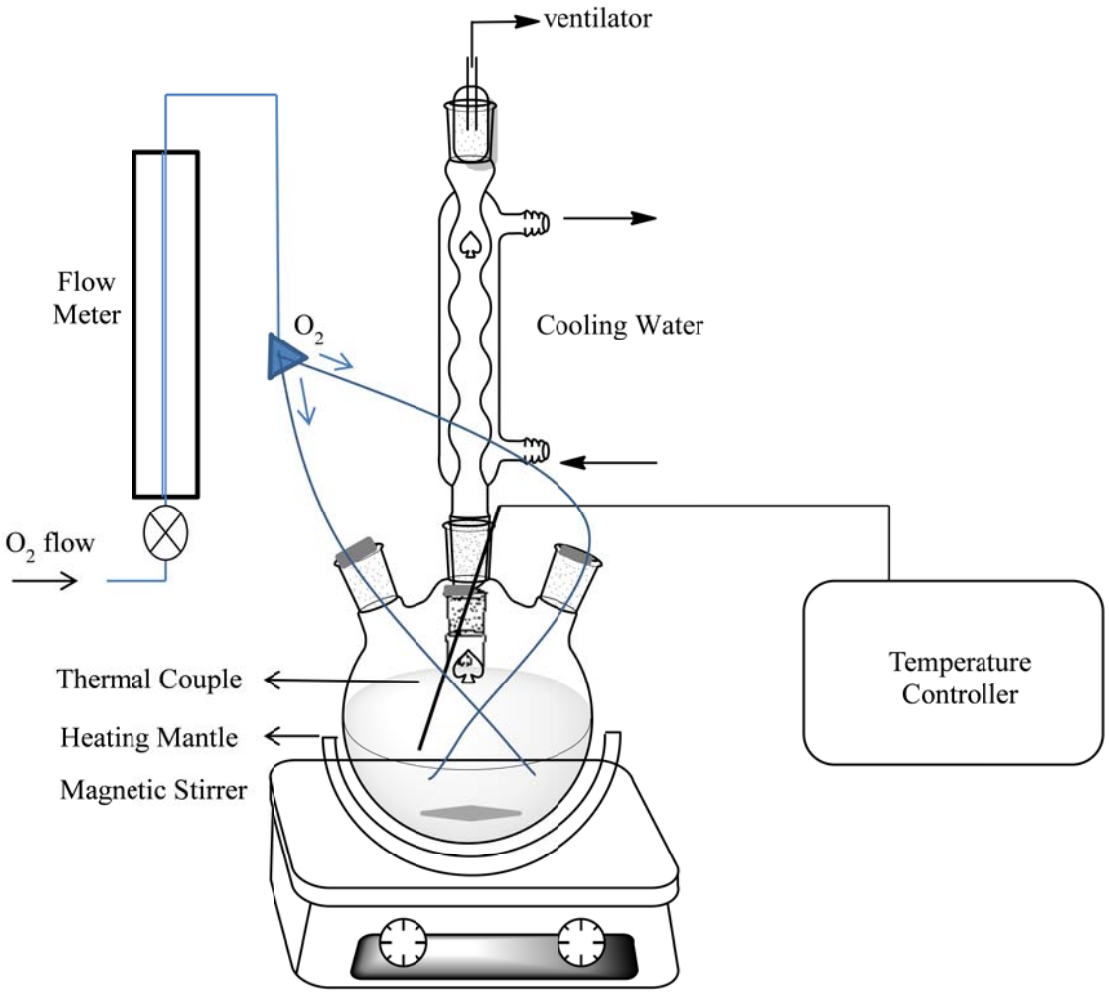

Figure 2.1 Scheme of reaction system for the oxidation of glycerol

Designated amounts of glycerol, H_2O and catalyst were measured and put into the four-necked flask. The system was assembled and heated to the designated temperature. After reaching the designated reaction temperature, the O_2 flow was turned on, and the timing of the reaction started. When the designated reaction time was reached, the O_2 flow was closed and the heating removed. A water bath was used to cool down the system. After reaching room temperature, the flask was removed from the system and the mixture was filtered through a Buchner funnel and washed with distilled water. The solution and catalyst were collected separately. The products in the solution were then analyzed by high performance liquid chromatography (HPLC).

During a typical sampling test, around 0.4 mL of the reaction mixture was taken out of the flask through a needle inserted in one of the rubber stoppers. The mixture was immediately filtered by using a Millex-LG-0.20 μm hydrophilic filter and tightly sealed in a 0.5 drams vial.

All the product solutions were kept in a refrigerator, as both glycerol and the potential products are perishable.

2.5 Product analysis

The products of the glycerol oxidation reaction were analyzed by a high performance liquid chromatography (HPLC) system. This HPLC system was composed of an Altech 426 pump, a Rheodyne 7725i sample injector, an Agilent Zorbax SAX separation column,

and a Linear UVIS 200 detector. Data were recorded through a Tekpower TP4000ZC digital multimeter interfaced to a personal computer.

Various set-ups and parameters were tested for the HPLC system, including a different pump, a refractive index (RI) detector, various eluent flow rates, various UV wavelengths, and various eluent recipes. The potential products and expected in the samples, including glycerol, dihydroxyacetone, glyceric acid, glyceraldehyde, tartronic acid, pyruvic acid, mesoxalic acid, lactic acid, oxalic acid, glycolic acid, acetic acid, formic acid, glyoxalic acid, and glyoxylic acid, were tested and confirmed by their retention time. Only dihydroxyacetone, glyceric acid, and glyceraldehyde were detected in most sample analysis. The following conditions were modified and proven the best in the fast separating and quantification of the products from the reactions in this thesis. The advantages and disadvantages of the excluded conditions are listed in the end of this section for future reference.

Eluent: Mixture of acetonitrile and phosphoric acid buffer. The volume ratio is $V_{acetonitrile}$: $V_{phosphoric\ acid\ buffer}$ = 2.5:1. The phosphoric acid buffer contains 5.8×10^{-3} mol/L H_3PO_4 and 3.0×10^{-3} mol/L NaOH in aqueous solution, for a final pH value of 2.2. The recipe was modified from Ref. [5]. Eluent flowrate: 1 mL/min. UV wavelength: 210 nm.

An external standard method was used to quantify the concentration of each product in the sample mixture. A series of standard solutions covering the concentration ranges of

the potential samples were prepared for each of the three main products. They were run under the same condition as the samples. Both the peak areas and the peak heights were used to obtain linear standard curves, which were forced to go zero crossing. The standard solutions were re-prepared and re-analyzed to obtain a new series of standard curves every time after the HPLC system was not used for months.

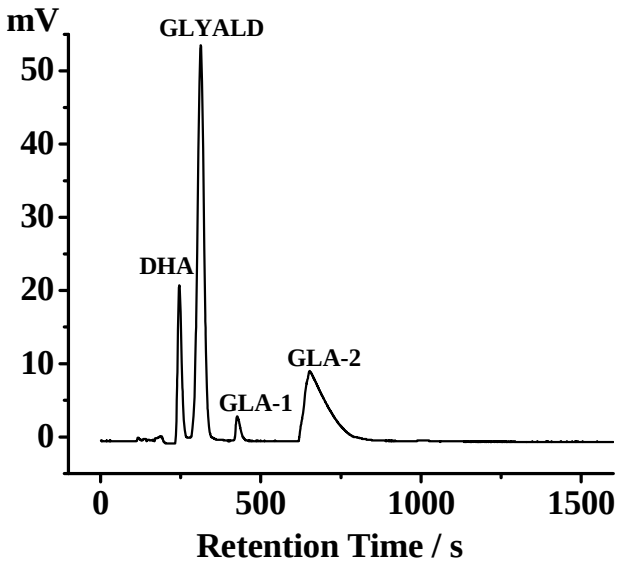

Figure 2.2 A typical HPLC chromatograph of glycerol oxidation product mixture

The reaction mixtures from the accumulated reactions were filtered, and diluted with water to 50.00 mL using a volumetric flask. If the pH value was not within the 2-to-7 range, the aliquot was neutralized or diluted to this designated pH range to avoid damage of the Zorbax SAX column. Usually 100 μL of the sample solution was injected into the HPLC system, and the measurement repeated three times to get more accurate results. The concentration of a given product in the 50 mL solution was then calculated by using

the standard calibration curve. The yield of this certain product was determined by the original amount of glycerol added into the system.

The product from the sampling test was measured by HPLC after filtration through the Millex-LG-0.20 μm hydrophilic filter, followed by dilution when necessary. Usually only one aliquot was analyzed due to the limited volume of each sample.

A typical HPLC chromatograph is shown in Figure 2.2. The four peaks in the chromatograph from left to right correspond to dihydroxyacetone (DHA), glyceraldehyde (GLYALD), and the two peaks for glyceric acid (GLA).

Potential modifications of the HPLC analysis for future reference may include the following:

(1) Pump and detector:

A refractive index (RI) detector was tested, accompanied by a Waters 510 pump, which could provide a reference line to the RI detector. The RI detector could be used by itself or in a series connection with the UV detector. The RI detector could detect potential products not easy to see with the UV detector, as well as glycerol. However, it is more than ten times less sensitive than the UV detector. With the available instrument, the signal/noise ratio is too low and the peaks too wide, and they overlap heavily. Therefore the RI detector was not used for our product analysis.

(2) Wavelength:

Wavelengths in the UV detector in the 170-450 nm range were tested for all the standard samples. A value of 210 nm was found to give the best signal/noise ratio and a good balance of peak intensity among the potential products. The glycerol peaks cannot be observed with 210 nm light, but can be observed with 190 nm light or even smaller wavelengths. However, with those wavelengths, the base-line gets very noisy, and the glycerol peak overlaps heavily with the glyceraldehyde peak and cannot be separated by adjusting the eluent recipe. Run of one sample under two wavelengths to deduct the peak area of the glyceraldehyde peak calculated from analysis with 210 nm light to calculate the concentration of glycerol was also tested. The result shows large errors, and therefore the method was deemed not feasible.

(3) Eluent recipe:

The current volume ratio of acetonitrile and phosphoric acid buffer used, and the concentration and the pH of the phosphoric acid buffer were carefully modified and proven to be the best for analyzing samples containing dihydroxyacetone, glyceraldehyde, and glyceric acid. The volume ratio largely affects the retention time, the peak width, and the degree of separation for all the products, while the concentration and the pH value of the phosphoric acid buffer mainly affect the retention time, the peak width, and the degree of separation of the acidic products. Our recipe may be subject to further modifications in the future if the reaction conditions are changed and new products appear in the sample.

2.6 References

[1] Y. Xia, Y. Xiong, B. Lim, S. E. Skrabalak, *Angew. Chem. Int. Ed.* **2009**, 48, 60-103.

[2] I. Lee, R. Morales, M. A. Albiter, F. Zaera, *Proc. Natl. Acad. Sci.* **2008**, 105, 15241-15246.

[3] I. Lee, F. Delbecq, R. Morales, M. A. Albiter, F. Zaera, *Nat. Mater.* **2009**, 8, 132-138.

[4] T. S. Ahmadi, Z. L. Wang, T. C. Green, A. Henglein, M. A. El-Sayed, *Science* **1996**, 272, 1924-1926.

[5] D. Liang, J. Gao, H. Sun, P. Chen, Z. Hou, X. Zheng, *Appl. Catal. B* **2011**, 106, 423-432.

Chapter 3

Preliminary exploration of glycerol oxidation kinetics

3.1 Introduction

Glycerol oxidation is a complex reaction system with reactants from liquid and gas phases, the catalyst and support in a solid phase, and the presence of solvent, under heating and stirring. There are many parameters that could potentially affect the selectivity of the reaction. In order to test its structure sensitivity, it is necessary to exclude some of these variables. A basic understanding of the reaction and proper experimental conditions is the premise to getting reliable result. In this chapter, knowledge about glycerol oxidation from the literature is briefly summarized, that constituted, the basis for the experiments carried out by us to determine the proper conditions for comparing Pt catalysts with different structures, the study that is discussed in the following chapter.

3.2 A literature overview

Indication of structure sensitivity in the catalytic system of glycerol oxidation from the literature has been briefly stated in 1.2.2. In this section, the main focus is on providing a comprehensive review of what is known about the reaction, including the catalyst preparation and pretreatment, the reaction condition, and the reaction process and mechanism.

The potential products of glycerol oxidation are listed in Figure 3.1. In the literature of glycerol oxidation catalyzed by heterogeneous catalyst, various metals have been tested, including Pt, Pd, Au, and bimetallic catalysts based on these metals. Supports have

included different kinds of carbon, silica, titania, alumina, and others. The reaction has generally been carried out in batch mode, either in glassware under atmospheric pressures or in an autoclave with higher pressure. Water has often been used as the solvent. The temperature has been varied from 20℃ to 100℃. Considerable conversion has been achieved under various conditions. The effect of each of these conditions will be summarized below.

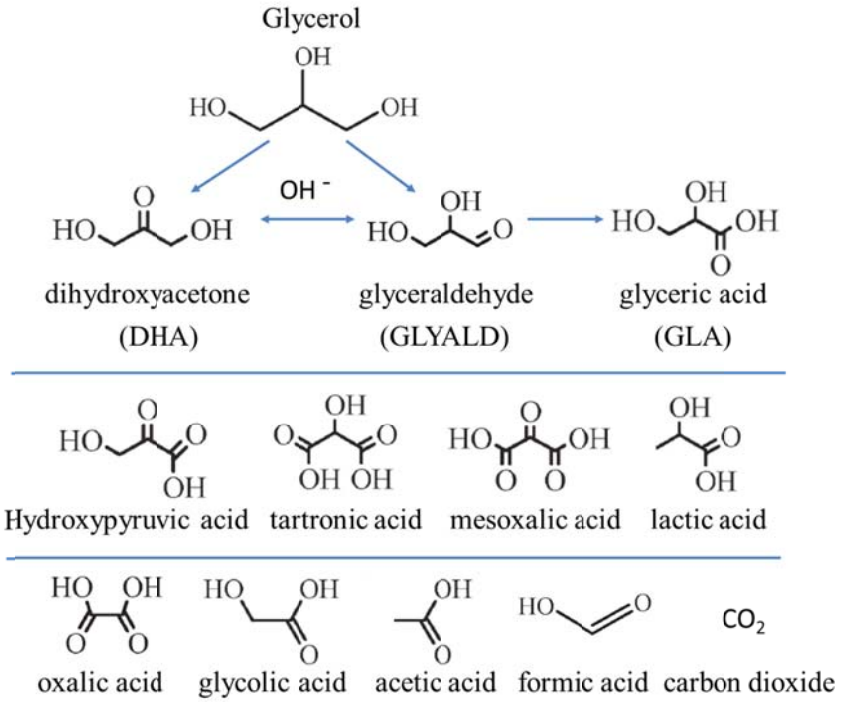

Figure 3.1 Potential products of glycerol oxidation

3.2.1 Metal

Pt and Pd were active catalysts for this reaction in neutral, and even slightly acidic, solutions, while Au is only active with the addition of a base such as NaOH or KOH. When pure Pt catalyst has been used, the oxidation reaction has shown to be relatively mild, with only few C1 and C2 products were observed. The main products have been

DHA, GLYALD, and GLA. Sometimes further oxidation products have been observed [9; 15], such as glycolic acid, tartronic acid, and oxalic acid. Pd often causes C-C bond cleavage. Au catalysts show higher selectivity toward GLA than Pd catalysts, but also promote deeper oxidation over GLA, and even C-C bond cleavage. In some cases, 100% GLA selectivity has been achieved [17]. Discussion on the selectivity of Au catalysts is abundant in the literature, but that has focused on the selectivity between GLA and further oxidation products, not on the selectivity between primary and secondary carbon reactivity in the first step of the oxidation. Other metals such as Re and Ru have also been tested but have not shown any significant activity for this reaction [2].

As stated in 1.2.2, this thesis focuses on Pt catalysts. Several studies have shown that Pt catalysts modified by Bi reverse the selectivity in primary/secondary carbon conversion. Kimura et al. [2] tested several promoters, including Bi, Te, Pb, Sb and Se, and found that Bi specifically shows a good performance by increasing the DHA yield. Compared to pure Pt/C catalysts, their optimized 1wt% Bi-5wt%Pt/C catalyst displayed increased selectivity for DHA, from 10% to 80%. Similar results were obtained by other researchers who tried to improve on the original recipe [6; 13-14]. The highest combination of conversion and selectivity was achieved by Garcia et al. [6] who reported 70-80% selectivity toward DHA after 70-80% of glycerol conversion.

The mechanism for this selectivity with Bi addition remains unclear. Kimura et al. [2] used CO adsorption experiment and XPS measurement to show that the Pt surface is

partially covered by Bi, and proposed that Bi functions as site blockers on Pt (111) planes and alters the adsorption orientation of glycerol on the Pt surface to favor the oxidation of the secondary hydroxyl group. This hypothesis was adopted by almost all of the follow-up researchers. Mallat et al. [4] agreed with the site blocking effect while also proposed that, under higher conversions, hydroxyl groups bond stronger on Bi than on Pt, suggesting that Bi may become an active site too. However, so far, there is no direct experimental evidence to prove these hypotheses.

3.2.2 Support

In heterogeneous catalysis, the role of the support is often very important. Properties of the support that may affect the performance of the catalyst include its surface area, pore structure, electronic structure, the interaction between the support and the metal, its redox and acid-base properties, and its stability under the reaction environment. For the glycerol oxidation, the use of various metal oxide support, including TiO_2, MgO, Al_2O3, V_2O_5, Nb_2O_5, Ta_2O_5, Fe_2O_3 and various carbon-based support, including carbon black, active carbon, graphite, and carbon nanotubes after different modifications, have been reported in the literature. For Pt catalysts, Gao et al. [10] showed that carbon nanotube-supported Pt displays higher activity than active carbon-supported Pt. Liang et al. [11] showed that carbon supports with various pretreatments result in Pt with different average sizes, and that such size differences affect the conversion and selectivity. For Au and bimetallic catalysts based on Au, Demirel-Gülen et al. [20] and Sobczak et al. [31] both showed that carbon supports result in higher activity than metal oxide supports, while Porta et al. [19]

and Derimel et al. [23] compared several kinds of carbon support and revealed that the pore structure also affects the catalytic behavior. Although metal oxide supports have generally shown less active than carbon supports, sometimes they had exhibit the benefit of providing alkalinity [29; 42] and better selectivity toward GLA [31].

3.2.3 Catalyst synthesis

Catalysts using different preparation methods have shown very different performance in glycerol oxidation [9; 17; 19-20; 23; 29; 35; 40]. However, the conclusions drawn from these studies have not been consistent. Different preparation methods usually lead to different particle size distributions, and also different potential residue molecules or elements left behind on the catalyst. These factors have not been isolated or singled out to study the influence of each one of them in the performance of the catalyst. The reported results have always included a combination of influences, and have thus not been easy to use to get a referable conclusion.

For Pt catalysts, Dimitratos et al. [9] reported that different preparation methods lead to different catalytic performance, with H_2 and $NaBH_4$ reduced Pt showing better activity and selectivity toward GLA than N_2H_4 reduced Pt. With Au catalysts, Carrettin et al. [17] showed that an Au/graphite catalyst with particle of sizes >50 nm are not active for the reaction. As for selectivity, Villa et al. [29] reported different activity for different sized catalyst but no selectivity differences, while Demirel-Gülen et al. [20] reported that

catalysts with smaller particles showed higher GLA selectivity; in contrast, Dimitratos et al. [35] showed larger particles have higher GLA selectivity.

3.2.4 O_2 pressure

O_2 is typically provided to the reaction mixture via bubbling under atmospheric pressureor by adding a certain initial pressure in an autoclave setup. Both air and pure O_2 have been used as the O_2 source, but pure O_2 has been used much more often. Increasing the O_2 pressure increases the concentration of O_2 dissolved in the solution. With Pt systems, Hu et al. [13] showed that as the O_2 pressure is increased from 0 to 180 psig, the reaction speed increases. However, the best DHA selectivity was achieved under 30-50 psig; lower or higher pressures resulted in lower DHA selectivity. In the case of Au, a similar pattern was observed, with an increase of O_2 pressure leading to an increase in the activity but high O_2 pressures also resulting in a decrease in GLA selectivity and an increase in further oxidation and C-C bond cleavage [7; 17; 44].

3.2.5 pH value

In all the reported work referring to this parameter, the addition of base was found to boost the activity of the Pt, Au, Pd, and bimetallic catalysts. Villa et al. [28] showed that, for Au catalysts, after the molar ratio of NaOH to glycerol reaches 2:1, further increases in the amount of NaOH result in very little increases in activity. As to the selectivity, in Pt systems, the selectivity toward DHA decreases with the increasing of pH [13]; while in Au systems, the selectivity for GLA production increases with the amount of base [17; 21;

28]. These results indicate that high pHs favor the formation of GLA over DHA, but also inhibit further oxidation of GLA to other acids.

3.2.6 Molar ratio of glycerol/catalyst

In the work of Carrettin et al. [17] and Villa et al. [28], the glycerol/metal ratio was studied with Au catalysts. They both showed that increasing the relative amount of catalyst lowers the GLA selectivity and promotes tartronic acid formation.

3.2.7 Temperature

Shen [44] has done kinetic studies on the effect of temperature on the activity and selectivity of glycerol oxidation. Elevated temperature increases the energy of reactant molecules while also inhibits the dissolution of O_2 in the solution, a factor that results in a deviation from the expected Arrhenius behavior. In a high-pressure closed system, the effect of temperature on the solubility of O_2 was shown to be relatively less critical than in an open atmospheric-pressure setup. Selectivity toward lactic acid production was found to increase with temperature, while the selectivity for GLA. Demirel-Gülen et al. [20] studied the Au catalyzed reaction from 20℃ to 100℃ and estimated the activation energy to be 50±5 kJ/mol.

3.2.8 Insights into the mechanism of the reaction

The mechanism for alcohol oxidation catalysis is still under discussion, but the common assumption is that it goes through an oxidative dehydrogenation step. It is assumed that

alcohols adsorb on the catalyst surface to form alcoholate species and then oxidize to their corresponding aldehyde or ketone [12]. Wörz et al. [12], based on the observeddeactivation of a Pt-Bi catalysts, proposed that since many of the products are strong chelating agents, their strong adsorption may block the active surface sites. Based on some kinetic experiments, they speculated that GLA blocks the active site that promotes DHA formation. With Au and Au-Pd bimetallic catalyst, Shen [44] measured the activation energy of the reaction and concluded that dehydrogenation to form intermediate species is the rate-determining step. They found that the GLA selectivity decreases rapidly above 60℃ while the E_a remains the same.

Zope et al. [45] have used isotope experiments to show that O_2 participate in the oxidation reaction not as O_2 or as radical O dissociated from O_2 directly but via the formation of *OH species resulting from interactions with H_2O on metal surfaces. They used DFT calculations to show that dehydrogenation steps appear to be largely promoted with the help of these *OH species and that, without the addition of NaOH, the dehydrogenation on Pt is easier than on Au. They concluded that the activity of the reaction depends on the concentration of *OH species on the metal surface, and that the concentration of *OH depends on the concentration of OH^- in the solution and the ability of the metal to accommodate extra negative charge.

3.3 Experimental result and discussion

In this section, we study the effect of several reaction parameters on the behavior of this catalytic reaction. The variables include temperature, O_2 flow rate, time, catalyst pretreatment, and number of trials. The experimental details for the glycerol oxidation have been described in Sections 2.4 and 2.5.

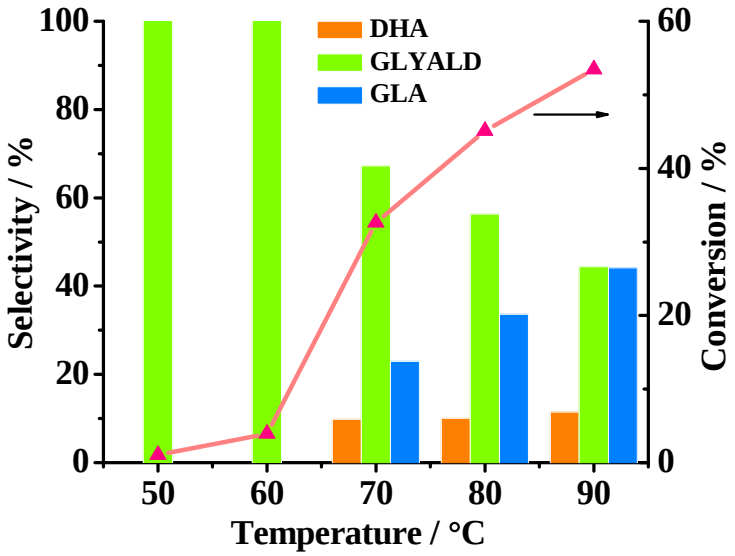

Figure 3.2 Effect of temperature on glycerol oxidation activity and selectivity upon catalysis with Pt/SiO_2 (Reaction conditions: homemade 1 wt% Pt/SiO_2 made by aqueous impregnation and calcination under 400℃ for 3 h, O_2 100 mL/min, 0.2 g glycerol in 2% aqueous solution, glycerol/Pt molar ratio = 500.)

3.3.1 Temperature

We tested the reaction under temperatures from 50℃ to 90℃ using a homemade 1 wt% Pt/SiO_2 catalyst. The results are shown in Figure 3.2. The conversion was seen to

increase with temperature, and a big leap was observed from 60℃ to 70℃. The accumulated conversion after 3 hours of reaction increases from 4.0% to 32.6% in this 10℃ temperature range. Although the activity keeps increasing at 80℃ and 90℃, in order to maintain the reaction condition as mild as possible while also consider the error in the product analysis, we chose 70℃ as the reaction temperature to be used for the structure-sensitivity experiments in the following chapters.

Three products have been observed in our reaction system: DHA, GLYALD, and GLA. The selectivity is shown in the histogram in Figure 3.2. Note that DHA is the product of secondary carbon oxidation while GLYALD and GLA both results from primary carbon oxidation. At low temperatures, only GLYALD was detectable, but as the temperature was increased the conversion and the selectivity of GLA were seen to also increase, with only a slight increase in DHA selectivity. This shows that the not only the overall conversion but also the conversion from GLYALD to GLA is affected by temperature.

3.3.2 O_2 flow rate

The O_2 flow rate was tuned from 10 mL/min to 200 mL/min. The results are shown in Table 3.1. An unexpected trend was observed. Although O_2 is one of the reactant, the conversion rate does not increase with O_2 flow rate. On the contrary, it was seen to even decrease a little. This shows that O_2 may inhibit the reaction. It was determined that the O_2 flow rates tried here are enough for the reaction. The selectivity toward DHA was also observed to decrease with the increase of O_2 flow rate.

Table 3.1 The effect of oxygen flow rate on glycerol oxidation catalyzed by Pt/SiO_2

O_2 flow (mL/min)	Conversion (%)	DHA selectivity (%)
10	43.6	18.0
100	41.3	16.8
200	37.4	15.3

(Reaction conditions: homemade 0.5 wt% Pt/SiO_2 made by ethanol impregnation, 70℃, 4h, 0.2 g glycerol in 2% aqueous solution, molar ratio of glycerol/Pt molar ratio = 1000)

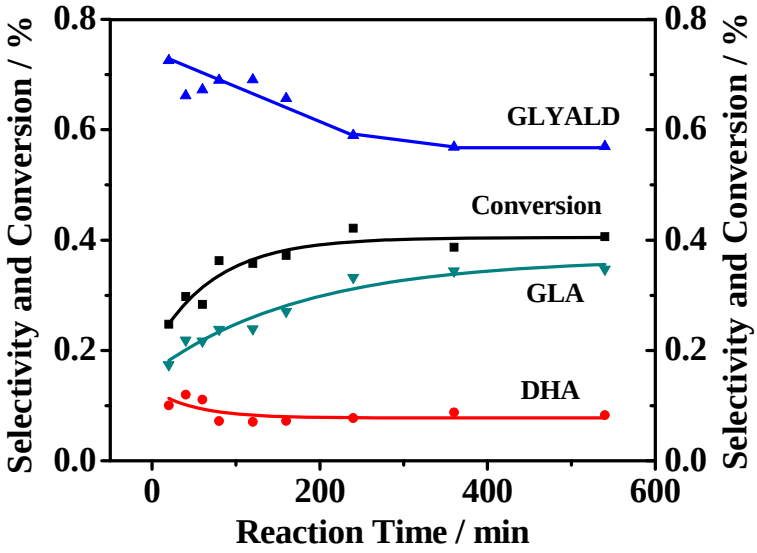

Figure 3.3 Conversion and selectivities vs. reaction time (reaction conditions: homemade 1wt% Pt/SiO_2, made by aqueous impregnation and calcination under 400℃ for 3 h, 70℃, O_2 flow = 100 mL/min, 0.2 g glycerol in 2% aqueous solution, glycerol/Pt molar ratio = 500)

3.3.3 Reaction time

The evolution of the conversion and product distribution vs. time is shown in Figure 3.3. These results were obtained from several different reaction kinetic experiments using the

same batch of catalyst but run for different reaction times. Only the final mixture was analyzed in each case; no intermediate aliquots were taken out during the reaction. The longest run was for 9 hours, but even then the conversion was seen to remain at ~ 40%, as after 4 hours of reaction. This shows that the reaction is completely inhibited after a certain point, indicating that the catalyst is deactivated during the reaction.

It should also be noted that the selectivities of all three products changes as the overall conversion increases during reaction. This suggests that the comparison of selectivities needs to be carried out under similar conversions. Otherwise, any data showing a different selectivity could well be due to the fact that they were acquired at different stages of the reaction, and may not be readily attributed to any intrinsic differences in the performance of the catalyst.

It can also be noted that, as the reaction proceeds, the selectivity for DHA, which is low initially, still decreases more, while the selectivity for GLYALD versus GLA changes significantly. It is very likely that the GLYALD gradually converts to GLA during the reaction, as GLYALD is expected to be much easier to oxidize than glycerol. It is also interesting to contrast the trend of DHA selectivity in the time and temperature series. The conversion was seen to increase with both with reaction time and temperature, but the DHA yield decreases with reaction time but increases with temperature. This phenomenon may indicate that the selectivity toward DHA production is likely related to the activity of the Pt/SiO_2 catalyst rather than to the extent of conversion. And as

indicated in the O_2 flow rate test, extra amount of O_2 flow deactivates the catalyst and also causes the selectivity toward DHA to decrease.

3.3.4 Catalyst pretreatment

A H_2 pretreatment was used to activate the catalysts. Pre-reduction is a common pretreatment for Pt catalysts. During the synthesis, the catalyst impregnated with H_2PtCl_6 is calcined under air. The precursor is expected to decompose at the high temperatures used, but may also partially oxidize; and pre-reduction is needed to reduce all Pt species. The results from our studies on this pre-treatment are shown in Table 3.2. After applying the H_2 pretreatment, there was always a large increase in catalytic activity. This confirms that the initial low conversion is due to Pt oxidation. The same H_2 pretreatment was applied to a commercial Pt/SiO_2 catalyst, which is already reduced during the manufacturing process. An opposite trend was observed in that case: the conversion decreased after the pretreatment. TEM images obtained before and after the treatment shows no aggregation occurred during the treatment (Figure 3.4). Therefore, changes in the oxidation state of the Pt in these catalysts may still be the most likely cause of the variations seen in catalytic performance. The reaction was also compared under a lower O_2 flow rate. There, contrary to the trend in Table 3.1, for the commercial Pt/SiO_2, a lower O_2 flow was seen to cause a decrease in catalyst activity. This indicates that O_2 does not cause catalytic deactivation in this case and facilitates the reaction on Pt catalysts with low oxidation states. These results suggest that neither over-oxidized catalysts nor over-reduced catalysts achieve the best activity. There seems to be a subtle

intermediate oxidation state for Pt that best facilitates the reaction. Further characterization data are needed to reach a final conclusion on this issue.

Table 3.2 Glycerol oxidation results vs. catalyst pretreatment

Catalyst	Conversion (%)	Yield (%)		
		DHA	GLYALD	GLA
Homemade – no treatment	13.8	1.4	9.4	3.0
Homemade – H_2 treatment	42.5	5.6	17.2	19.6
Commercial – no treatment	44.2	5.4	22.7	16.1
Commercial – H_2 treatment	31.2	4.9	19.1	7.2
Commercial – lower O_2 flow	35.0	4.2	21.0	9.9

(Reaction conditions: 1wt% Pt/SiO_2, 70℃, 3 h, O_2 flow = 100 mL/min, 0.2 g glycerol in 2% aqueous solution, glycerol/Pt molar ratio = 500; H_2 treatment: 350℃, 3 h, pure H_2 flow = 20 mL/min)

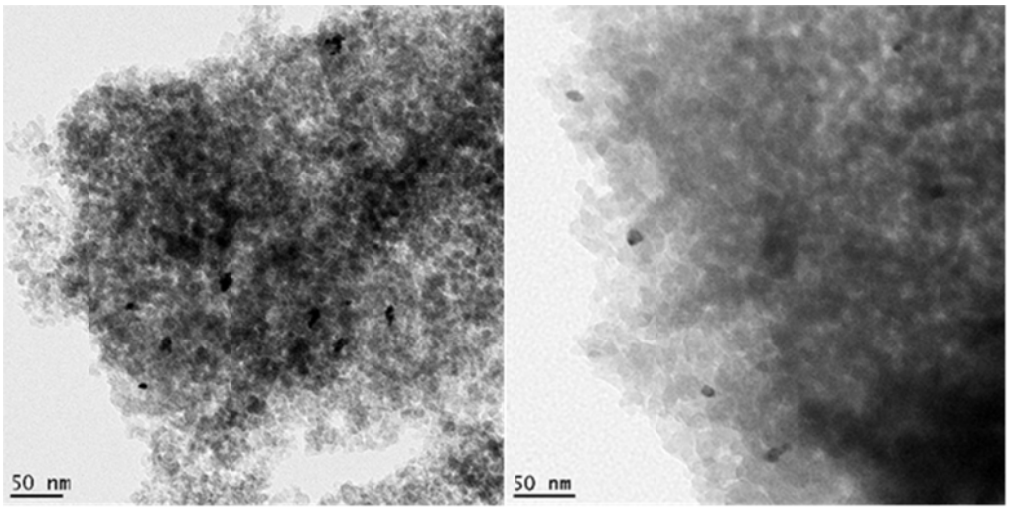

Figure 3.4 TEM images for the commercial 1% Pt/SiO_2 catalyst before and after 350℃ H_2 treatment.

The important role that an intermediate oxidation state for the metal may play in catalytic activity can be explained by the role of surface species in the reaction. As stated in 3.2.8, Zope et al. [45] have shown that adsorbed *OH species facilitate the conversion of alcohols to aldehydes, and that the coverage of *OH depends on the ability of the metal to accommodate negative charges. If the Pt is in a zero oxidation state, the surface *OH concentration may be low, and that may inhibit the reaction. On the other hand, a highly oxidized Pt surface with a higher concentration of *OH may probably hinder the adsorption of the reactants. The glycerol molecule has three hydroxyl groups and would compete for adsorption sites with the surface *OH species. Pt surfaces in moderate oxidation states may provide enough *OH species for the reaction but not to the extent that the adsorption of the reactant is hindered, and therefore is expected to be the best for the reaction.

This understanding also provides some clues on the possible origins of the selectivity differences seen for this reaction with surface structure. Under similar oxidation states, close-packed surfaces may favor an adsorption state of glycerol with less spatial hindrance, namely, in a linearly adsorbed form, which should favor the formation of GLYALD. In contrast, the edge and step sites of the metal nanoparticles offer less spatial hindrance, and should therefore favor an adsorption state with a higher adsorption energy, a chelating adsorbed glycerol. For this adsorption conformation, from both kinetic and thermodynamic points of view (electronic effects for hydrogen removal and stability of the product), DHA should be the favored product. In Bi-doped Pt system, Bi probably

increase the chance of chelating adsorption of glycerol by creating extra steps and edges on the Pt surface. If so, high-index facets may show a more notable difference in selectivity. Further characterization of the adsorption forms of glycerol on different surfaces is necessary to test this explanation.

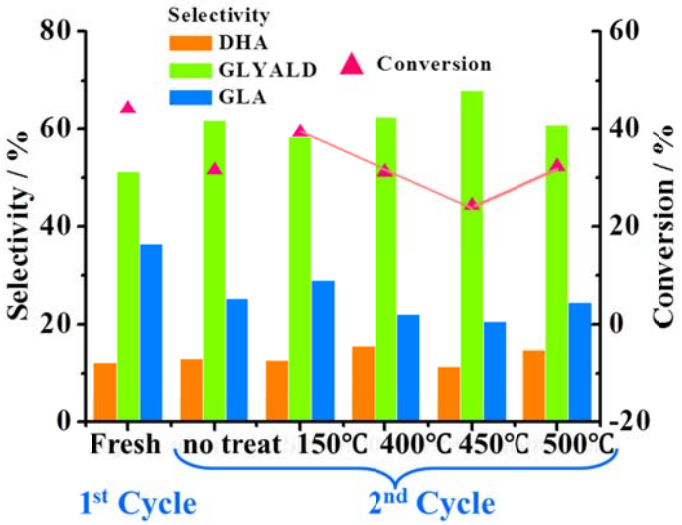

Figure 3.5 Catalyst recycling test (Reaction conditions: commercial 1wt% Pt/SiO_2, 70℃, 3 h, O_2 100 mL/min, 0.2 g glycerol in 2% aqueous solution, glycerol/Pt molar ratio = 500; H_2 treatments: 150℃ 1 h; 400-500℃ 3 h, pure H_2 flow = 20mL/min)

3.3.5 Catalyst recycling test

The possibility of recycling the Pt/SiO_2 catalyst after reaction was tested next. The results are shown in Figure 3.5. After filtration, if the catalyst was used again without any further treatment in between, a decline in its activity was observed (as shown in the second column). Possible reasons for this deactivation include: (1) the catalyst being oxidized

during the reaction; (2) strong adsorbates covering the active surface sites; and (3) Pt nanoparticle aggregation during the reaction.

As considered above, the oxidation of the metal is a likely reason for its deactivation. Therefore, H_2 treatments were also tested after recycling of the catalyst. The third to the sixth columns in Figure 3.5 show the results on catalytic activity and selectivity with catalysts obtained after heating in H_2 flow at 150, 400, 450, and 500℃. 1 h of H_2 treatment at 150℃ does restore part of the initial activity and leads to a higher conversion than with the catalyst without this treatment. However, further increases in H_2 treatment temperature or treatment time were found to not increase the activity further, as the Pt particles might aggregate during such treatments. Selectivities for DHA, GLYALD, GLA production show some differences among these trials, but these selectivities were measured under different total conversions, and the differences seems to follow the trend shown in Figure 3.3, with DHA and GLYALD selectivities decreasing with conversion while the GLA selectivity increases. There is no obvious indication of selectivity differences due to catalyst treatment between runs in the accumulated reaction results in Figure 3.5.

In conclusion, the catalyst activity decreases after reaction, meaning that the recycled catalyst cannot be used as is, without pretreatment, in any activity tests. On the other hand, mild H_2 treatments are suitable to regain catalytic activity.

3.3.6 DHA poisoning effect

The effect of DHA on glycerol oxidation is shown in Table 3.3. When DHA was added to the system, the conversion decreased a lot. Also the selectivity toward DHA itself was lowered with the existence of DHA. This indicates that the addition of DHA partially deactivates the catalyst. DHA formation is likely one of the reasons for catalyst deactivation observed in glycerol oxidation. The selectivity of DHA is observed to be positively related with catalyst activity again. When pure DHA was used as the reactant, trace amount of GLYALD was observed in the final mixture but the amount was too small to quantify. This shows that the conversion from DHA to GLYALD under this condition is very limited.

Table 3.3 The effect of DHA on glycerol oxidation catalyzed by Pt/SiO_2

Reactant	Conversion (%)	DHA selectivity (%)	Yield (%)		
			DHA	GLYALD	GLA
Glycerol	45.4	11.8	5.4	21.3	18.8
Glycerol + DHA*	26.2	8.6	2.3	17.0	6.9
DHA	-	-	-	-	-

(Reaction conditions: 1wt% Pt/SiO_2, 70℃, 3 h, O_2 flow = 100 mL/min, 0.2 g glycerol in 2% aqueous solution, glycerol/Pt molar ratio = 500. *DHA/glycerol molar ratio = 0.08)

3.4 Conclusion

In this chapter, some basic information was acquired on the effect of some basic parameters on the performance of glycerol oxidation reactions catalyzed by Pt/SiO_2 catalysts, and proper conditions were established for selectivity comparison to use in the

following chapters. Reaction conditions such as temperature, O_2 flow rate, reaction time, and catalyst pretreatment were shown to exert a significant influence on the activity and selectivity of the catalyst. Consequently, comparisons of selectivity need to be carefully carried out under the same reaction conditions. Otherwise, the observed differences may not be attributable to the structure of the Pt catalyst. The catalyst was also shown to become partially deactivated during the reaction; recycled catalysts cannot be used as fresh catalysts to compare selectivity.

The products observed in this study include DHA, GLYALD and GLA, showing that both primary and secondary carbons can be oxidized in our system. The selectivity changes observed with time and temperature indicate a possible relation between catalyst activity and DHA selectivity. Based on the analysis of existing data and the current knowledge provided in literature, it can be stated that close-packed surface are expected to favor primary carbon oxidation, and open surfaces secondary carbon oxidation.

3.5 References

[1] H. Kimura, *Appl. Catal. A* **1993**, 105, 147-158.

[2] H. Kimura, K. Tsuto, *Appl. Catal. A* **1993**, 96, 217-228.

[3] T. Mallat, A. Baiker, *Catal. Today* **1994**, 19, 247-284.

[4] T. Mallat, Z. Bodnar, P. Hug, A. Baiker, *J. Catal*. **1995**, 153, 131-143.

[5] P. Fordham, M. Besson, P. Gallezot, *Appl. Catal. A* **1995**, 133, L179-L184.

[6] R. Garcia, M. Besson, P. Gallezot, *Appl. Catal. A* **1995**, 127, 165-176.

[7] S. Carrettin, P. McMorn, P. Johnston, K. Griffin, C. J. Kiely, G. J. Hutchings, *Phys. Chem. Chem. Phys*. **2003**, 5, 1329-1336.

[8] C. L. Bianchi, P. Canton, N. Dimitratos, F. Porta, L. Prati, *Catal. Today* **2005**, 102-103, 203-212.

[9] N. Dimitratos, C. Messi, F. Porta, L. Prati, A. Villa, *J. Mol. Catal*. **2006**, 256, 21-28.

[10] J. Gao, D. Liang, P. Chen, Z. Hou, X. Zheng, *Catal. Lett*. **2009**, 130, 185-191.

[11] D. Liang, J. Gao, J. Wang, P. Chen, Z. Hou, X. Zheng, *Catal. Comm*. **2009**, 10, 1586-1590.

[12] N. Wörz, A. Brandner, P. Claus, *J. Phys. Chem. C* **2010**, 114, 1164-1172.

[13] W. Hu, D. Knight, B. Lowry, A. Varma, *Ing. Eng. Chem. Res*. **2010**, 49, 10876-10882.

[14] D. Liang, S. Cui, J. Gao, J. Wang, P. Chen, Z. Hou, *Chin. J. Catal*. **2011**, 32, 1831-1837.

[15] D. Liang, J. Gao, H. Sun, P. Chen, Z. Hou, X. Zheng, *Appl. Catal. B* **2011**, 106, 423-432.

[16] Z. Lin, H. Chu, Y. Shen, L. Wei, H. Liu, Y. Li, *Chem. Commun*. **2009**, 7167-7169.

[17] S. Carrettin, P. McMorn, P. Johnston, K. Griffin, G. J. Hutchings, *Chem. Commun*. **2002**, 696-697.

[18] S. Carrettin, P. McMorn, P. Johnston, K. Griffin, C. J. Kiely, G. A. Attard, G. J. Hutchings, *Top. Catal*. **2004**, 27, 131-136.

[19] F. Porta, L. Prati, *J. Catal*. **2004**, 224, 397-403.

[20] S. Demirel-Gülen, M. Lucas, P. Claus, *Catal. Today* **2005**, 102-103, 166-172.

[21] G. J. Hutchings, S. Carrettin, P. Landon, J. K. Edwards, D. Enache, D. W. Knight, Y. Xu, A. F. Carley, *Top. Catal*. **2006**, 38, 223-230.

[22] S. Demirel, M. Lucas, J. Wärnå, T. Salmi, D. Murzin, P. Claus, *Top. Catal*. **2007**, 44, 299-305.

[23] S. Derimel, K. Lehnert, M. Lucas, P. Claus, *Appl. Catal. B* **2007**, 70, 637-643.

[24] W. C. Ketchie, Y. Fang, M. S. Wong, M. Murayama, R. J. Davis, *J. Catal*. **2007**, 250, 94-101.

[25] W. C. Ketchie, M. Murayama, R. J. Davis, *Top. Catal*. **2007**, 44, 307-317.

[26] E. Taarning, A. T. Madsen, J. M. Marchetti, K. Egeblad, C. H. Christensen, *Green Chem*. **2008**, 10, 408-414.

[27] B. N. Zope, R. J. Davis, *Top. Catal*. **2009**, 52, 269-277.

[28] A. Villa, D. Wang, D. Su, L. Prati, *Chem. Cat. Chem*. **2009**, 1, 510-514.

[29] A. Villa, A. Gaiassi, I. Rossetti, C. L. Bianchi, K. van Benthem, G. M. Veith, L. Prati, *J. Catal.* **2010**, 275, 108-116.

[30] A. Villa, G. M. Veith, L. Prati, *Angew. Chem*. **2010**, 122, 4601-4604.

[31] I. Sobczak, K. Jagodzinska, M. Ziolek, *Catal. Today* **2010**, 158, 121-129.

[32] K. Musialska, E. Finocchio, I. Sobczak, G. Busca, R. Wojcieszak, E. Gaigneaux, M. Ziolek, *Appl. Catal. A* **2010**, 384, 70-77.

[33] A. Takagaki, A. Tsuji, S. Nishimura, K. Ebitani, *Chem. Lett*. **2011**, 40, 150-152.

[34] N. Dimitratos, F. Porta, L. Prati, *Appl. Catal. A* **2005**, 291, 210-214.

[35] N. Dimitratos, J. A. Lopez-Sanchez, D. Lennon, F. Porta, L. Prati, A. Villa, *Catal. Lett.* **2006**, 108, 147-153.

[36] D. Wang, A. Villa, F. Porta, D. Su, L. Prati, *Chem. Commun*. **2006**, 1956-1958.

[37] W. C. Ketchie, M. Murayama, R. J. Davis, *J. Catal*. **2007**, 250, 264-273.

[38] A. Villa, C. Campione, L. Prati, *Catal. Lett*. **2007**, 115, 133-136.

[39] M. Sankar, N. Dimitratos, D. W. Knight, A. F. Carley, R. Tiruvalam, C. J. Kiely, D. Thomas, G. J. Hutchings, *Chem. Sus. Chem*. **2009**, 2, 1145-1151.

[40] N. Dimitratos, J. A. Lopez-Sanchez, J. M. Anthonykutty, G. Brett, A. F. Carley, R. C. Tiruvalam, A. A. Herzing, C. J. Kiely, D. W. Knight, G. J. Hutchings, *Phys. Chem. Chem. Phys.* **2009**, 11, 4952-4961.

[41] N. Dimitratos, A. Villa, L. Prati, Catal. Lett. **2009**, 133, 334-340.

[42] G. L. Brett, Q. He, C. Hammond, P. J. Miedziak, N. Dimitratos, M. Sankar, A. A. Herzing, M. Conte, J. A. Lopez-Sanchez, C. J. Kiely, D. W. Knight, S. H. Taylor, G. J. Hutchings, *Angew. Chem. Int. Ed.* **2011**, 50, 1-4.

[43] Y. Shen, S. Zhang, H. Li, Y. Ren, H. Liu, *Chem. Eur. J*. **2010**, 16, 7368-7371.

[44] Y. Shen, *studies on the selective catalytic oxidation of glycerol*, *Doctoral Dissertation*, Peking University, **2009**.

[45] B. N. Zope, D. D. Hibbitts, M. Neurock, R. J. Davis, *Science* **2010**, 330, 74-78.

Chapter 4

Size and shape effect in Pt in glycerol oxidation

4.1 Pt catalyst with different nanoparticle sizes

4.1.1 Accumulated reaction

Pt catalysts with various particle sizes were tested for the promotion of glycerol oxidation. The easiest and most reliable way to get different particle size while keeping the other conditions the same is to change the Pt loading during synthesis. Pt/SiO_2 catalysts were synthesized by the aqueous impregnation method using $H_2PtCl_6 \cdot 6H_2O$ with Pt loadings varying from 0.2 wt% to 10 wt%. All catalysts were calcined at 400℃ for 4 hours under air. The resulting catalysts were then reduced under H_2 flow at 350℃ for 3 hours before reaction. Four catalysts: 0.2wt%, 1wt%, 5wt%, and 10wt% Pt/SiO_2 were used for the glycerol oxidation reaction kinetic studies. The results after 3 hours are shown in Figure 4.1. The amount of glycerol and the glycerol/Pt molar ratio were kept the same in these reactions, while the amount of Pt/SiO_2 catalyst was adjusted based on their loading.

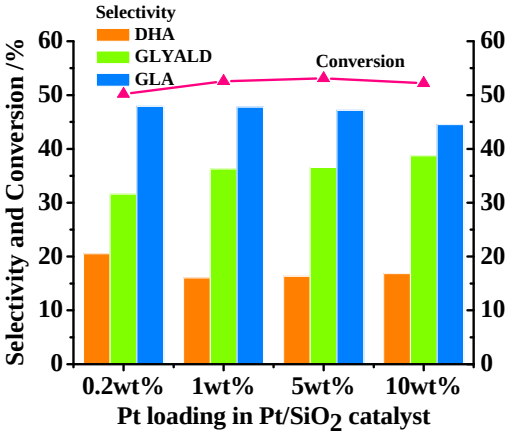

Figure 4.1 Conversion and selectivity in glycerol oxidation using Pt/SiO_2 catalysts with different metal loadings. (Reaction conditions: Pt/SiO_2 calcined and reduced, 70℃, 3 h, O_2 flow = 100 mL/min, 0.2 g glycerol in 2% aqueous solution, glycerol/Pt molar ratio = 500).

The measured conversions were almost the same with all these catalysts, but the selectivities of the three products were different, and showed an obvious trend: increases in Pt loading lead to slight decreases in the selectivity for DHA and GLA and an increase in GLYALD production. The selectivity difference between the 0.2 wt% Pt loading catalyst and the rest is relatively larger: the DHA yield and GLA/GLYALD ratio are higher than with the other catalysts.

TEM images for these catalysts are shown in Figures 4.2, and the average Pt particle sizes and size distributions extracted from those are reported in Figure 4.3. The average Pt particle size was seen to increase with Pt loading: the average sizes of the 0.2, 1, 5, and 10 wt% Pt/SiO_2 were 3.9, 4.9, 5.5, and 5.7 nm, respectively. The 0.2 wt% Pt/SiO_2 catalyst exhibits a narrow size distribution, whereas the others show relatively wide size distributions, with most of the Pt particles having diameters between 2 and 12 nm. The differences in the distribution in this size range is what caused the slight increases in average particle sizes seen with loading amount. The Pt particles were all well dispersed on SiO_2 without large aggregation. The shapes were mostly irregular.

Correlated with the observed selectivity trend, this structure information of the catalysts may indicate that smaller particles favor the formation of DHA and also promotes the conversion from GLYALD to GLA, while the larger particles favor the formation of GLYALD.

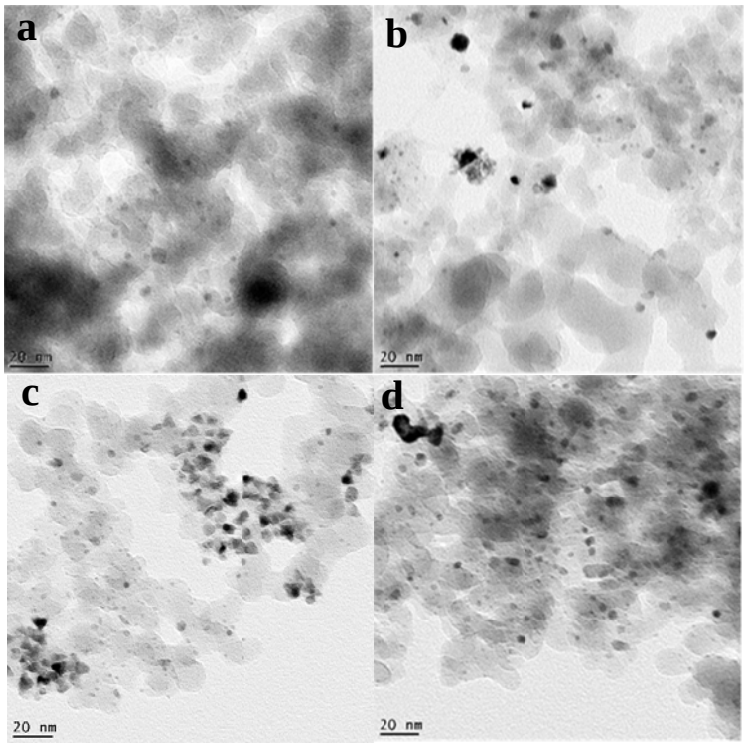

Figure 4.2 TEM images for Pt/SiO_2 with various Pt loadings.

(a. 0.2 wt% Pt/SiO_2; b. 1 wt% Pt/SiO_2; c. 5 wt% Pt/SiO_2; d. 10 wt% Pt/SiO_2).

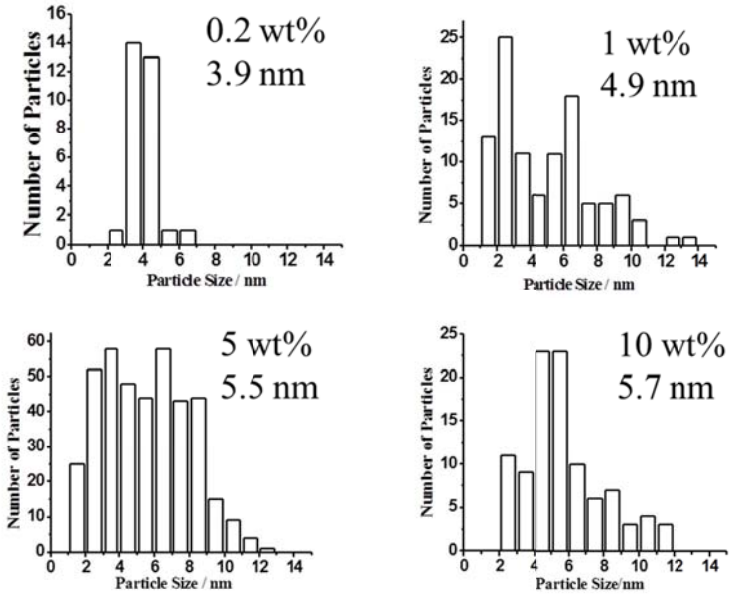

Figure 4.3 Average Pt particle sizes and size distributions for Pt/SiO_2 catalysts with various Pt loadings.

4.1.2 Sampling test

The kinetic results reported in Figure 4.1 correspond to accumulated conversion and selectivity data after 3 hours of reaction. Based on the discussion on the effect of conversion on catalytic performance discussed in the previous chapter, it was determined that it was necessary to observe the behavior of the catalysts throughout the course of the reaction. Accordingly, sampling tests were performed on these catalysts as a function of reaction time. Because the low density of the Pt/SiO_2 catalysts leads to the easy generation of static electricity, adding catalyst during reaction is likely to cause large errors, so the catalysts were added to the reactor before heating, and the point when the temperature reached 70℃ was used as the zero point for the kinetic measurements; the O_2 flow was initiated at that time. Samples were taken at 0, 1, 5, 10, 15, 20, 30, 60, 120, 180 and 240 min.

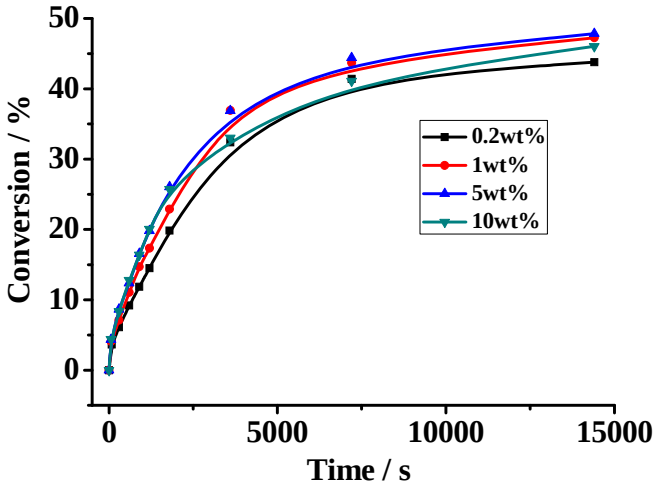

Figure 4.4. Conversion vs. Time for the glycerol oxidation reaction using Pt/SiO_2 catalysts with various Pt loadings (Reaction conditions: Pt/SiO_2 calcined and reduced, 70℃, 4 h, O_2 flow = 100 mL/min, 0.5 g glycerol in 2% aqueous solution, glycerol/Pt molar ratio = 1000)

The conversion changes versus time measured with all four catalysts are shown in Figure 4.4. The final conversions reached with the 0.2, 1, 5, and 10 wt% Pt/SiO_2 catalysts were 41%, 45%, 44%, and 43% respectively. The trends were similar to those obtained from the initial accumulated reaction experiments (Figure 4.1). 0.2 wt% Pt/SiO_2 catalyst with the lowest average Pt particle size shows the lowest conversion. This is unusual, as in all the reactions the molar ratio of glycerol to Pt was kept the same, and the number of surface Pt atoms is expected to decrease with the increase in average particle size. This indicates that the reaction rate is not the same on all surface Pt sites, and that the conversion does not decrease monotonically with particle size. As glycerol is a relatively large molecule, it could be argued that it may require surface sites of a certain dimension for the reaction to happen.

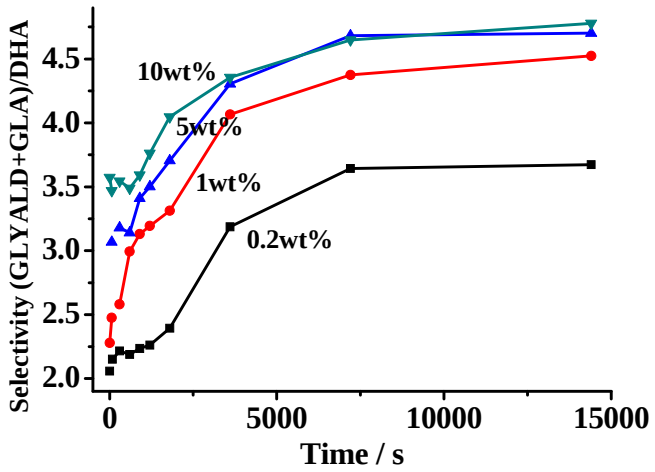

Figure 4.5. Selectivity vs. Time for the glycerol oxidation reaction using Pt/SiO_2 catalysts with various Pt loadings (Reaction conditions: Pt/SiO_2 calcined and reduced, 70°C, 4 h, O_2 flow = 100 mL/min, 0.5 g glycerol in 2% aqueous solution, glycerol/Pt molar ratio = 1000)

The evolution of the selectivity of the reaction versus time for the four catalysts is shown in Figure 4.5. The vertical coordinate is the ratio of the yields from oxidation of the primary (GLYALD and GLA) over secondary (DHA) carbons (referred to as 1C/2C hereinafter). In contrast to the results for the total activity, clear monotonic trends were observed here: the selectivity for primary carbon oxidation increased with Pt loading, namely, with Pt particle size, and a similar evolution in selectivity was observed during the course of the reaction with all these four catalysts, with the selectivity for primary carbon oxidation increasing markedly with time. As concluded in Chapter 3, any comparisons of selectivity should be carried out under similar conversion. Therefore, the selectivity changes with conversion are shown in Figure 4.6. The trends mentioned above become even clearer in that format: the selectivity toward primary carbon oxidation clearly increases monotonically with both Pt particle size and conversion.

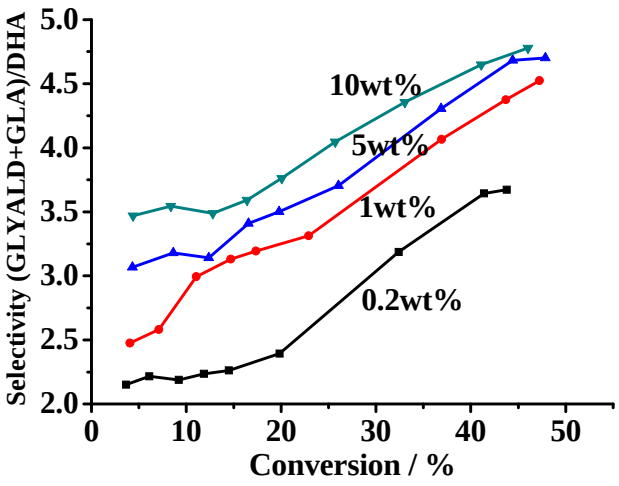

Figure 4.6 1C/2C Selectivity vs. Conversion for glycerol oxidation using Pt/SiO_2 catalysts with various Pt loadings (Reaction conditions: Pt/SiO_2 calcined and reduced, 70°C, 4 h, O_2 flow = 100 mL/min, 0.5 g glycerol in 2% aqueous solution, glycerol/Pt molar ratio = 1000)

As the selectivity of the catalyst changes during the reaction, the initial selectivity of these catalysts was also contrasted. The ratios of the initial rate of 1C oxidation over the initial rate of 2C oxidation, obtained from the slope of the tangent at time zero, are shown in histogram form in Figure 4.7 to better reflect the intrinsic selectivity of the catalyst. This new plot clearly shows the trend in increasing 1C/2C selectivity with Pt particle size, which clearly exists even at the very beginning of the reaction.

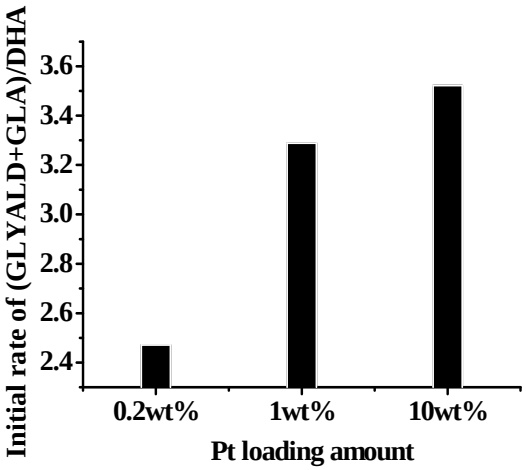

Figure 4.7. Ratio of the initial rate of the 1C product over the initial rate of the 2C product versus Pt loading (Reaction conditions: Pt/SiO_2 calcined and reduced, 70℃, 4 h, O_2 flow = 100 mL/min, 0.5 g glycerol in 2% aqueous solution, glycerol/Pt molar ratio = 1000)

The evolution of the reaction rate vs. time obtained with the 1 wt% Pt/SiO_2 catalyst is shown in Figure 4.8 in the form of turnover frequency (TOF), calculated from the slope of the yield-time curve and normalized by the total number of Pt atoms, not the surface Pt atoms; the curves for the other catalysts showed similar trends. It can be seen there that the rates for DHA and GLYALD formation both decrease with time, while the rate for GLA formation goes through a maximum at an intermediate (~2000 s) time. The latter

observation is typical of secondary, sequential, reactions: GLA is produced via oxidation of GLYALD, and the rate of that conversion depends on the concentration of primary GLYALD product. The yield of GLYALD actually increases over time regardless, and the decrease in GLA formation rate at later times may be due to deactivation of the catalyst.

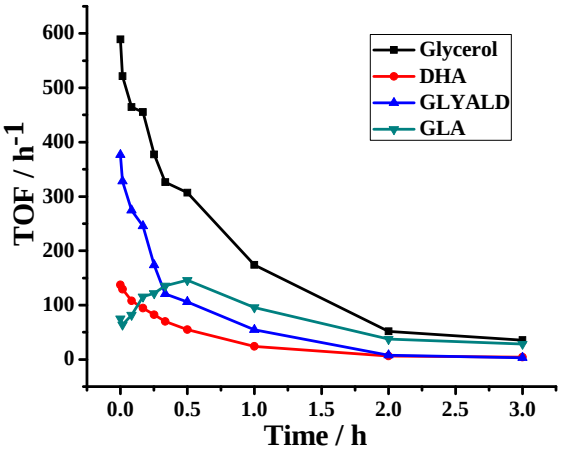

Figure 4.8 Reaction rate vs. Time of 1 wt% Pt/SiO_2 in glycerol oxidation (Reaction condition: Pt/SiO_2 calcined and reduced, 70℃, 4 h, O_2 flow = 100mL/min, 0.5 g glycerol in 2% aqueous solution, molar ratio of glycerol/Pt = 1000)

In conclusion, a clear trend in selectivity with Pt particle size has been observed under strictly controlled experimental conditions. For Pt/SiO_2 catalysts with average particle sizes varying from 3.9 nm to 5.7 nm, selectivity toward primary carbon oxidation increases monotonically with Pt particle size and conversion.

4.1.3 Pt surface characterization

To further learn about the surface structure of the catalysts and correlate that information with their selectivity and activity, CO-IR titration experiment experiments were performed on the catalysts as a function of metal loading. About 14 mg of each powder catalyst was pressed to make a translucent pellet. Those sample pellets were dried at 150℃ under vacuum for at least 30 min, and then pretreated with three O_2/H_2 cycles under 350℃ in the IR cell. 200 Torr of O_2 or H_2 were used, each treatment lasting for 1 hour. 10 Torr of CO was then introduced at -160℃, and kept in the IR cell volume for 10 min before pumping it away. Typical spectra obtained for the CO adsorbed on the catalyst as the sample was warmed up are shown in Figure 4.9. The peak at 2100 cm^{-1} is assigned to CO adsorbed on Pt surface in atop sites [1]. As temperature was increased, the peak was seen to move slightly to lower wavenumbers, a reflection of a slight decrease in surface coverage [1]. A second broader peak was also seen at 1890 cm^{-1} and assigned to CO adsorbed on Pt surface sites in a bridge conformation on low coordination sites [1]. This peak position did not change with temperature. The peak position and shift trend vs. temperature was the same for all four catalysts. The weak peak seen at 2350 cm^{-1} was due to CO_2 peak.

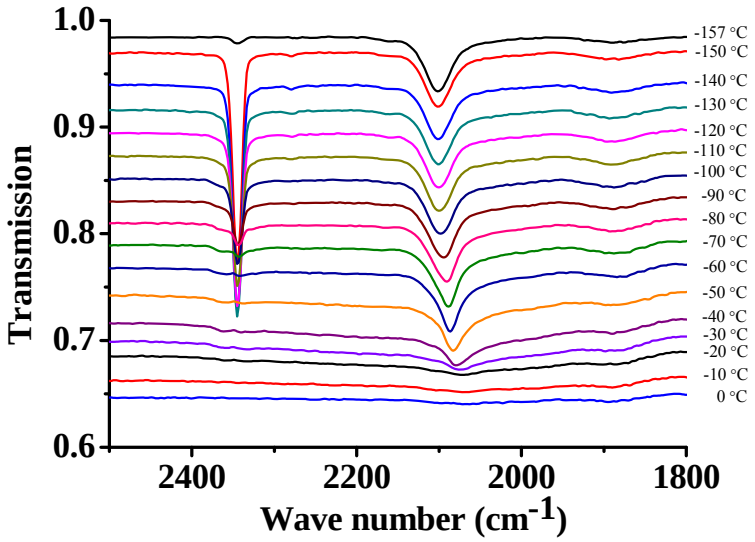

Figure 4.9 IR spectra for 1 wt% Pt/SiO_2 after being exposed to CO (Experimental conditions: Vacuum = 10^{-2} Torr, 14 mg catalyst/pellet, dried at 150℃ for 0.5 h and pretreated with O_2/H_2 at 350℃, CO 10 Torr for 10 min, vacuum for 15 min).

The transmission IR spectra were converted to absorbance spectra and the two absorbance peaks were integrated to obtain the peak areas. The results are shown in Table 4.1. The reproducibility of the peak area was not good among the same samples, even though the same amounts of catalyst from the same batch were used. In order to make the quantification of the results comparable, KBr was used to dilute the Pt/SiO_2 catalysts with the higher metal loadings in order to keep the amount of Pt the same in the pellet. Unfortunately, no CO peak was observed in those cases, maybe because the high density of the pellets made it hard for CO to diffuse and adsorb onto the Pt inside the pellets. Nevertheless, clear trends are still observed in Table 4.1, with increasing CO uptake in the atop sites (and to a lesser extent in the bridge sites as well) with increasing loading, in

particular with the 10 wt% sample. Also, the coverage of the bridge sites seem to amount to approximately 10% of the atop sites for all samples except the one with 0.2 wt% Pt, for which the ratio is much higher; this catalyst may have a much larger fraction of high-coordination adsorption sites. All this behavior can be easily justified by the concomitant increase in particle size, because larger nanoparticles tend to expose larger low-Miller-index terraces where these CO adsorbed species form. It can be concluded that the larger Pt particles expose an increase fraction of flat surfaces. If the reproducibility problem in these measurements could be solved, the peak position, intensity and ratio between CO-top and CO-bridge peak could provide more quantitative information about the Pt surface sites.

Table 4.1. CO IR absorption peak areas (in arbitrary units) from CO adsorbed on Pt/SiO_2 catalysts with various Pt loadings at -160℃ (14 mg catalyst/pellet)

	CO-top ($2210\text{-}1963 cm^{-1}$)	CO-bridge ($1963\text{-}1800 cm^{-1}$)
0.2 wt%	0.30	0.14
1 wt%	1.13	0.16
	1.16	0.19
	2.12	0.24
	1.87	0.30
5 wt%	6.04	0.63
	9.19	0.90
10 wt%	29.30	2.96

4.1.4 Reproducibility and size controlled synthesis

Since the size distributions of the Pt nanoparticles in our catalysts were relatively large, it is likely that both the average size and the size distribution may have played a role in defining the selectivity of the glycerol oxidation. The wide size distributions seen here may also affect the reproducibility of the catalyst. In order to clarify how the catalyst structure affects the selectivity and activity, detailed kinetic experiments are needed to obtain information of reaction mechanism, with high reproducibility being a necessity. Therefore, it was determined necessary to improve on the synthesis of these catalysts in order to obtain samples with narrow size distributions in a highly reproducible way. Additionally, in order to obtain a proper particle size series, Pt catalysts with several average sizes were needed, all with narrow size distributions and synthesized under similar conditions. Although Pt catalysts have been widely used in the literature, almost no reported catalyst synthesis procedure readily satisfies this requirement.

We have tested several methods for Pt-based catalysts, and found that an ethanol impregnation method is better than others in reproducibility test. The size information of Pt/SiO_2 catalysts prepared by ethanol impregnation with Pt loading amounts varying from 0.2 wt% to 1 wt% is shown in Table 4.2. To distinguish them from the Pt/SiO_2 prepared by aqueous impregnation, they are referred to as Pt/SiO_2-E hereinafter. The TEM images and size distributions estimated from those are shown in Figure 4.10(a, b, c), and Figure 4.11(a, b, c), respectively. From the TEM images, it was determined that the Pt particles are irregular in shape but display size distributions much sharper than those obtained with

the catalysts prepared using the aqueous impregnation method. A test of the calcination temperature used to tune particle size was also carried out, from which the data shown in Table 4.2, entries 2 to 6, were obtained: the average Pt particle size was seen to increase with calcination temperature, but small particles, of about ~ 1 nm in diameter, were still detected in al samples, and the size distributions were seen to significantly overlap. Using the ethanol impregnation method, when the Pt loading amount reached 1 wt%, the size distribution was seen to spread out extensively: the Pt particle sizes of the 1 wt% Pt/SiO_2 expanded from 2.1 nm to 8.8 nm, and also overlapped significantly with those of the Pt/SiO_2 catalysts with lower loadings. An additional 1 wt% Pt/SiO_2 sample was prepared using $Pt(NH_3)_4Cl_2$ as the precursor and a pH-controlled aqueous impregnation (1 wt% Pt/SiO_2-N hereinafter), and that sample was seen to display a larger average particle size, approximately 8.5 nm. A TEM image of this catalyst and its size distribution are also shown in Figures 4.10 (d) and 4.11 (d), respectively. Although the size distribution was relatively large compared to those for the 0.2 wt% and 0.5 wt% Pt/SiO_2 samples, it was much narrower than the ones for the 1 wt% to 10 wt% Pt/SiO_2 catalysts prepared from $H_2PtCl_6 \cdot 6H_2O$ by the aqueous impregnation method. The distribution also overlapped to a much lesser extent with those of the 0.2 wt% to 1 wt% Pt/SiO_2 cases, as shown in Figure 4.11.

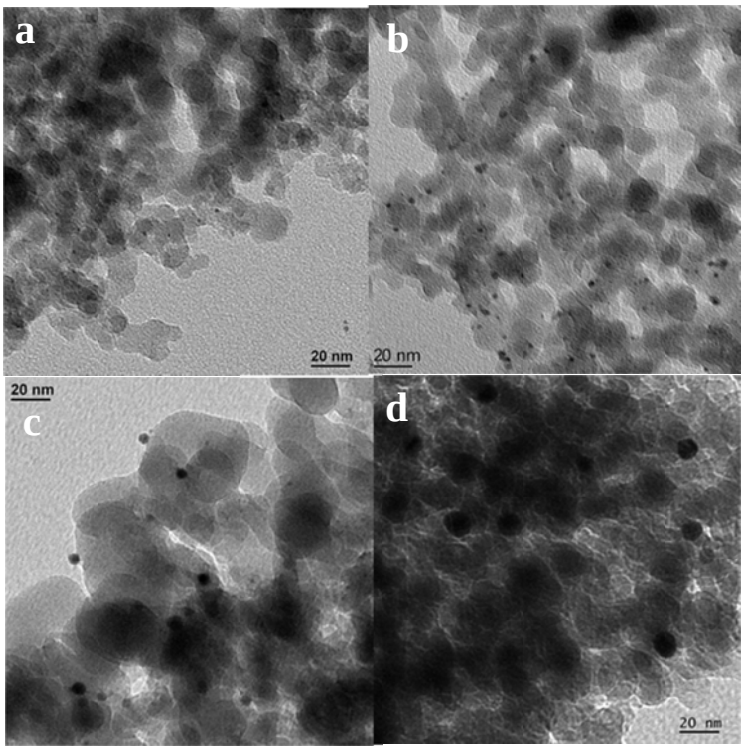

Figure 4.10. TEM images for the newly-prepared Pt/SiO_2 size series, calcined and reduced under 200℃ (a. 0.2 wt% Pt/SiO_2-E; b. 0.5 wt% Pt/SiO_2-E; c. 1 wt% Pt/SiO_2-E; d. 1 wt% Pt/SiO_2-N).

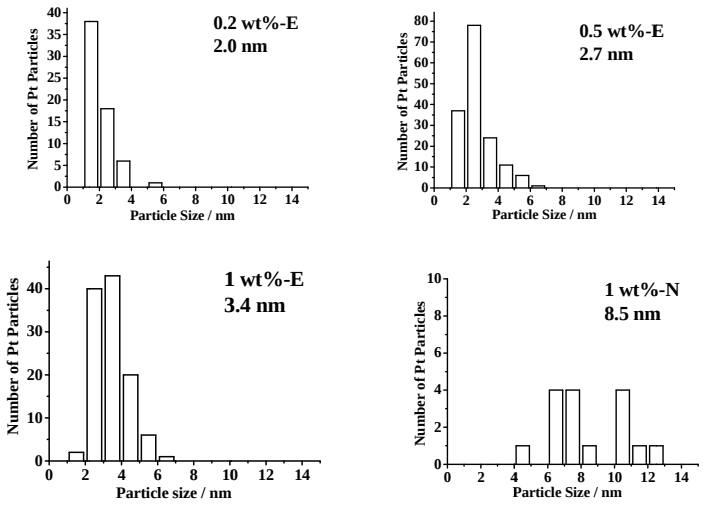

Figure 4.11. Average particle sizes and size distributions for the newly-prepared Pt/SiO_2 size series, calcined and reduced under 200℃ (a. 0.2 wt% Pt/SiO_2-E; b. 0.5 wt% Pt/SiO_2-E; c. 1 wt% Pt/SiO_2-E; d. 1 wt% Pt/SiO_2-N).

Table 4.2. Summary of Pt particle size information for the Pt/SiO_2 catalysts prepared using $H_2PtCl_6 \cdot 6H_2O$ and an ethanol impregnation method.

Catalyst	Pt wt%	Calcination T/℃	Average size/nm	Standard deviation/nm	Largest/nm	Smallest/nm	Counts
Pt/SiO_2	0.2	200	1.9	0.5	4.8	1.1	77
Pt/SiO_2	0.5	200	2.2	0.4	3.0	1.2	55
Pt/SiO_2	0.5	300	1.9	0.8	4.6	0.7	188
Pt/SiO_2	0.5	400	2.1	0.6	3.9	1.0	117
Pt/SiO_2	0.5	500	2.9	0.9	5.7	1.6	61
Pt/SiO_2	0.5	600	3.1	1.2	8.0	1.0	126
Pt/SiO_2	1	400	4.6	1.5	8.8	2.1	181

The newly prepared catalysts were tested for the glycerol oxidation reaction. Several parallel experiments were carried out to test their reproducibility. If the catalyst showed good reproducibility in terms of the accumulated yield at the end of the catalytic runs, namely, if the standard deviation among several trials were no larger than 5%, the samples were then tested further by following the kinetics over time, taking liquid samples along the way. The 0.5 wt% Pt/SiO_2 catalyst prepared by ethanol impregnation showed the best reproducibility, and could be used for more kinetic experiments in the future.

The kinetic results from experiments with the new catalyst size series for glycerol oxidation are shown in Figure 4.12. The final conversions obtained with the 0.2 wt%, 0.5 wt% and 1 wt% Pt/SiO_2-E samples were 47%, 47%, and 45%, respectively, while the conversion with the 1 wt% Pt/SiO_2-N was only 23%, about half of those obtained with the other catalysts. In addition, the 1C/2C selectivity no longer displayed the monotonic increase with conversion reported before, and in terms of particle size, the relative trends

follow the same direction but the absolute values did not mesh with the old data (Figure 4.13). More experiments are needed to resolve these inconsistencies. The discrepancy showed in Figure 4.13 may indicate that small adjustments in the synthesis process may affect the selectivity to a large extent. The higher 1C selectivity is probably caused by ethanol induced during the synthesis.

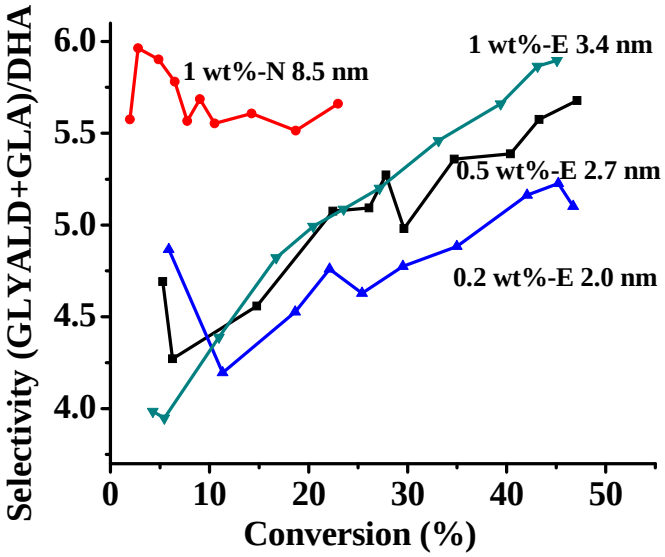

Figurer 4.12. Selectivity vs. conversion for glycerol oxidation using the newly-prepared Pt/SiO_2 size series (Reaction conditions: 70℃, 4 h, O_2 flow = 100 mL/min, 0.5 g glycerol in 2% aqueous solution, glycerol/Pt molar ratio = 1000.)

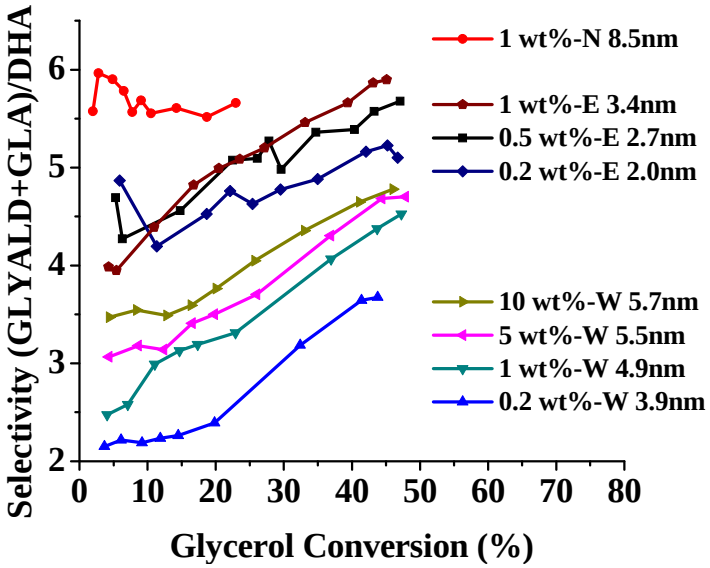

Figure 4.13. Combined selectivity vs. conversion plots obtained with the two Pt/SiO_2 size series (Reaction conditions: 70℃, 4 h, O_2 flow = 100mL/min, 0.5 g glycerol in 2% aqueous solution, glycerol/Pt molar ratio = 1000.)

4.2 Pt catalysts with different nanoparticle shapes

4.2.1 Catalyst synthesis

Tetrahedral and cuboctahedral shaped Pt nanoparticles (T-Pt and C-Pt hereinafter, respectively) were synthesized by following the procedure and recipe described in 2.2.2. To reduce any effects originating from other molecules and ions induced in the synthesis, an aqueous solution H_2 reduction method was used to synthesize the Pt nanoparticles. TEM images obtained for the T-Pt and C-Pt nanoparticles are shown in Figure 4.14. The size of the T-Pt nanoparticles was estimated to be 6.7 ± 1.2 nm, while that of the C-Pt nanoparticles was measured as 9.0 ± 0.9 nm. The particle size varied slightly among

different synthetic batches. The T-Pt colloidal nanoparticles were protected by PVP, and the C-Pt colloidal nanoparticles were protected by SPA.

The next step in our catalyst synthesis was to disperse the shaped nanoparticles onto the SiO_2 support and to remove the protecting surfactant to expose the well-defined crystal facets. Direct filtration was tried first, to get rid of the organic matter in solution. However, that only worked for the T-Pt nanoparticles. In the case of the C-Pt nanoparticles, the filtrate solution still had the color of the nanoparticles, indicating that the interaction between the C-Pt nanoparticle and the SiO_2 surface was not sufficiently strongly for the latter to retain the former. Centrifugation was also tested to separate the nanoparticles from the polymer solution, but because the nanoparticles are quite small, this did not work properly, and insufficient separation led to unknown Pt nanoparticle losses during solvent replacement. In the end, a method was established based on the use of rotary evaporation to dry the solution. The mixture was evaporated under vacuum and in a 75℃ water bath.

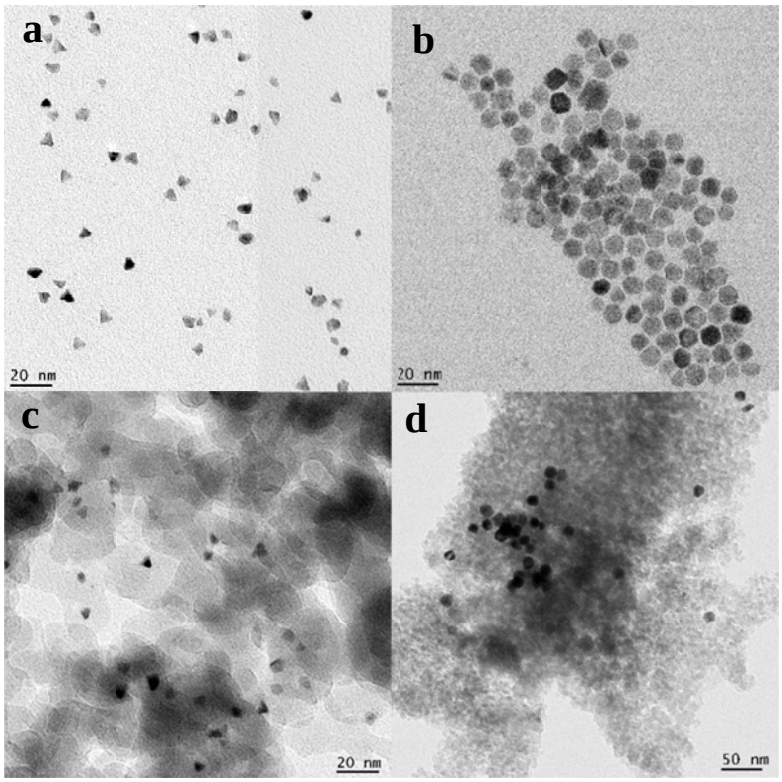

Figure 4.14. TEM images of shape controlled Pt nanoparticles, by themselves and after dispersion on a silica support (a. T-Pt colloidal nanoparticles; b. C-Pt colloidal nanoparticles; c. 1 wt% T-Pt/SiO_2; d. 1 wt% C-Pt/SiO_2)

4.2.2 Catalytic performance

The performance of these new catalysts with well-defined Pt nanoparticle shapes was first tested in solution directly. The kinetic results for the oxidation of glycerol are shown in Figure 4.15. A black precipitate was observed to develop with the T-Pt system after 10 min of reaction, and the conversion increased slightly still afterwards. In contrast, the C-Pt catalyst remained stable throughout the reaction. Although the overall conversion was only around 5%, both T-Pt and C-Pt colloidal nanoparticle solutions did show activity for

glycerol oxidation. The low conversions were likely due to the protecting polymers around the Pt nanoparticles inhibiting the access of glycerol molecule to Pt surface.

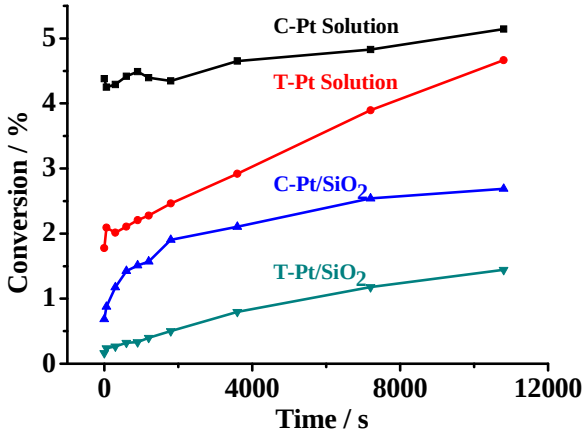

Figure 4.15. Conversion vs. time curves obtained for the glycerol oxidation reaction using the T-Pt and C-Pt catalysts, by themselves and dispersed on a silica support (Reaction conditions: 70℃, 3 h, O_2 flow = 100 mL/min, 0.5 g glycerol in 2% aqueous solution, glycerol/Pt molar ratio = 1000).

The supported T-Pt/SiO_2 and C-Pt/SiO_2 were also tested for the glycerol oxidation without any pretreatments. The results are shown in Figure 4.15. Both catalysts displayed lower activity after dispersion onto the SiO_2 support, probably because of a reduction in accessibility to the surface after loading the nanoparticles onto the support. The C-Pt nanoparticles displayed higher conversion than the T-Pt both before and after dispersion. The evolution of these reactions in terms of selectivity is shown in Figure 4.16, together with the Pt loading amount series. Both T-Pt/SiO_2 and C-Pt/SiO_2 catalysts showed higher 1C selectivity than the regular Pt/SiO_2 samples, regardless of metal loading. C-Pt/SiO_2

showed higher 1C selectivity than T-Pt/SiO_2. This is probably due to the Pt particle size and the protecting polymers. The polymers on the surface of both C-Pt and T-Pt catalyst may cause a large steric hindrance for the adsorption of glycerol on Pt surface. Therefore, primary carbons are likely to get close to the surface easier than secondary carbons and lead to the high selectivity toward primary carbon oxidation products.

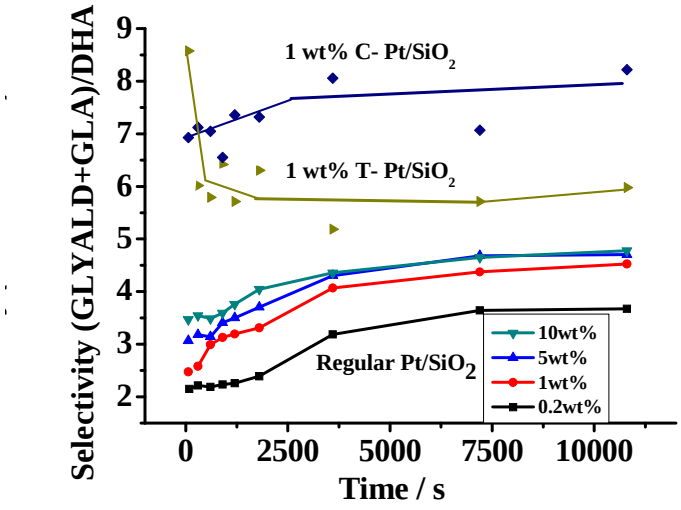

Figure 4.16. Selectivity vs. time for glycerol oxidation using the T-Pt/SiO_2, C-Pt/SiO_2 catalysts, reported together with the data for the regular Pt/SiO_2 catalysts (Reaction conditions: 70℃, O_2 flow = 100 mL/min, 0.5 g glycerol in 2% aqueous solution, glycerol/Pt molar ratio = 1000).

As the T-Pt/SiO_2 and C-Pt/SiO_2 nanoparticles are both protected by the surfactants used in their synthesis, their activity was found to be relatively low compared to those of the regular Pt/SiO_2 catalysts. In order to remove the protecting polymers, O_2 and H_2 cycling pretreatment were applied to the T-Pt/SiO_2 sample, which was calcined at 300℃ for three O_2/H_2 cycles each consisting of 30 min calcination under 20 mL/min of O_2 and 30 min

exposure to 20 mL/min of H_2. Due to the limited amount of catalyst available, the molar ratio of glycerol to Pt in the kinetic studies was chosen to be to 5000 instead of 1000, while the concentration of glycerol in the solution was kept the same (0.2 wt%). The TOFs measured in these experiments are shown in Figure 4.17. The initial TOFs measured for the pretreated T-Pt/SiO_2 catalyst was found to be much higher than those seen with the catalyst without treatment: a 20-fold increase in the initial rate was seen after the pretreatment was applied. This shows that the O_2/H_2 pretreatment to remove the surface polymers and increase accessible to the Pt surface is very effective. However, the deactivation of this catalyst was also quite fast. This is very likely due to the small amount of catalyst used in the reaction system, which would lead to a faster deactivation process, or perhaps because of Pt sintering. The TEM image obtained for the T-Pt/SiO_2 after the pretreatment shown in Figure 4.18 shows that some of the particles were rounded after the treatment, indicating that the use of a temperature of 300℃ for 3 hours may be too stringent for this catalyst. No aggregation was observed, however. Milder treatments shall be tested in the future.

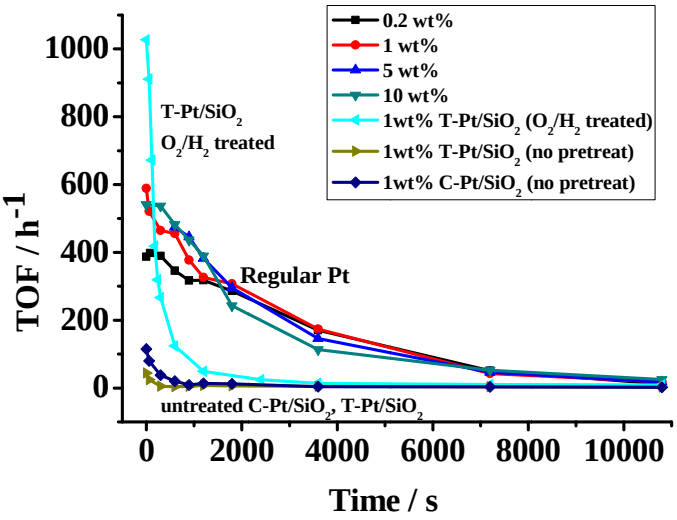

Figure 4.17. Reaction rate vs. time from glycerol oxidation experiments with the shape- and size-controlled Pt/SiO_2 catalysts (Reaction conditions: Pt/SiO_2 calcined and reduced, 70℃, O_2 flow = 100 mL/min, 0.5 g glycerol in 2% aqueous solution, glycerol/Pt molar ratio = 1000 for the regular catalysts, 5000 for the pretreated $T\text{-}Pt/SiO_2$ sample)

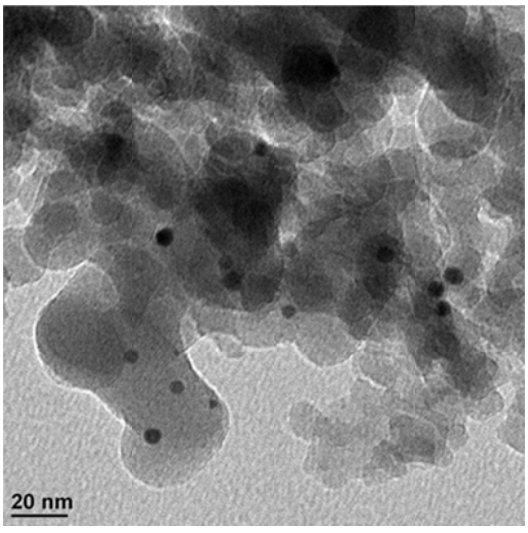

Figure 4.18 TEM image from the $T\text{-}Pt/SiO_2$ after an O_2/H_2 thermal pretreatment.

4.3 Conclusion

In this chapter, Pt catalysts with varies particle size and shape have been tested in the glycerol oxidation reaction under strictly controlled conditions and structure sensitivity of this reaction has been identified. Selectivity toward the oxidation of primary carbon has been observed to increase monotonically with Pt particle size. With the structure information provided by TEM and CO IR titration experiment, these results appear to indicate that larger Pt particles with flat surfaces may promote primary carbon oxidation, whereas edge, corner, and other low-coordination Pt sites may promote secondary carbon oxidation. Reproducibility and particle size control of Pt/SiO_2 catalyst has been improved by modifying the catalyst synthesis to an ethanol impregnation method. However, small adjustment in the synthesis process shows large effect to the selectivity. Catalysts prepared from similar synthetic method with narrow size distribution, good reproducibility, and covering a larger size range are needed to improve and confirm the result. Tetrahedral- and cuboctahedral-shaped Pt have also been tested and cuboctahedral-shaped Pt exhibits higher activity and higher selectivity toward primary carbon oxidation before removing the protecting polymers. O_2/H_2 treatment is proved to be effective in removing the polymers but more mild conditions shall be tested in the future to avoid shape transformation. The result of well-shaped Pt catalyst needs to be confirmed in more detail.

4.4 References

[1] N. Sheppard, T. T. Nguyen, The vibrational spectra of carbon monoxide chemisorbed on the surface of metal catalysts—A suggested scheme of interpretation. In Advances in Infrared and Raman Spectroscopy; R. J. H. Clark, R. E. Hester, eds. Heyden, London, **1978**, 5, 67-148.

Chapter 5

Conclusions and future work

5.1 Conclusions

In conclusion, we have observed that the structure of the Pt particles in Pt/SiO_2 catalysts affects their activity and selectivity in the oxidation of glycerol. Using Pt/SiO_2 catalysts prepared by an aqueous impregnation method with various Pt loadings and particle sizes, varying from 3.9 to 5.7 nm, it was seen that the selectivity toward the oxidation of the primary carbon increases monotonically with Pt particle size. We also observed that in all these catalysts, the preference for primary carbon oxidation increases during the reaction, and that deactivation of the catalyst happens at the same time. The deactivation is very likely due to oxidation and DHA. Together with the CO IR titration results, these results appears to indicate that larger Pt particles with flat surfaces and extensive fractions of atop and bridge sites may promote primary carbon oxidation, whereas edge, corner, and other low-coordination Pt sites may promote secondary carbon oxidation. Further catalyst characterization and kinetic experiments will be needed to confirm this tentative conclusion. Tetrahedral- and cuboctahedral-shaped Pt catalysts were also tested for the glycerol oxidation reaction, and cuboctahedral-shaped Pt nanoparticles were found to display higher activity and higher selectivity toward primary carbon oxidation. These catalysts require careful pretreatment to remove the surface surfactants used in their synthesis while keeping the Pt particle shapes, and that needs to be studies in more detail to confirm the trends reported here.

5.2 Suggestions for future work

We conclude by offering some suggestions for future work:

1. To improve on and confirm the information extracted from the studies with the Pt size series, better control needs to be exercised over the Pt particle size while keeping the synthetic method the same. It has been shown that slight changes in synthetic methodology may significantly affect the performance of the final catalyst. The following two sets of experiments may be performed (others may be developed in the future):

(a) Changes the Pt loading may be varied within a larger range by using the ethanol impregnation method or other well-controlled synthesis with good reproducibility. However, the making of larger nanoparticles this way may result in larger size distributions. It shall be noted that when the size distribution is wide, the results most likely reflect the behavior of the particles in the whole size range rather than the behavior of the particles with the average size, and that may be dominated by a particular minority size range.

(b) Use of a seed growth method. The current seeding methods in the literature either lack a good control on the amount of metal used or involve too many other molecules in the system. In preliminary tests of a seeding method with the T-Pt colloidal nanoparticles, it was seen that adding more Pt after the seed formation results in Pt particle with similar sizes until the tetrahedral shape is changed to a tetrapod structure in higher Pt concentrations. In any case, seed growth may also work for other Pt nanoparticle synthetic systems. It should be kept in mind that the nature of the surfactant used, the reduction agent, and the solvent should be kept the same in these syntheses, all other

molecules and ions shall be removed from the solutions used as much as possible, and the amount of Pt used shall be accurately determined and measured.

2. Shaped-controlled Pt catalysts shall be tested when the surface polymers are completely removed. Other O_2/H_2 treatment conditions and various methods such as UV-O_3 treatments may be tested for this catalyst cleaning. CO-IR titration and high resolution TEM experiments could be used to characterize the final Pt surface structures and correlate those with their performance in the glycerol oxidation reaction.

3. Reproducibility shall be strictly confirmed for each of the catalysts used in the nanoparticle size and nanoparticle shape catalyst series. As shown by our result, the variations in reaction selectivity with Pt particle size may not be monotonic. To confirm the trend reported here, more data points are needed, covering a larger size range and showing higher reproducibility. Accurate surface characterization and kinetic experiments all have high requirements in terms of the reproducibility of the catalyst being used.

4. To clarify how the structure of the Pt surface affects the selectivity of the glycerol oxidation, the reaction mechanism shall be explored. Kinetic experiments could be carried out in terms of pressure and concentration dependences and with similar reactants to explore the effect of the three known products and/or other possible intermediates present in solution on the catalyst and the reaction. The coverages of the different Pt

surface sites could be estimated by using the result from CO-IR and HRTEM studies on well-controlled Pt catalyst to correlate with their behavior. The adsorption conformations of the glycerol, the products, and the intermediates on Pt surfaces may be hard to determined (perhaps this can be done under UHV conditions, but also worth trying, since those very likely lead to the selectivity difference observed in catalysis.

5. Based on the current results from this work, it could be speculated that larger Pt nanoparticles may promote primary carbon oxidation while edge and corner Pt sites may promote secondary carbon oxidation. The oxidation state of the surface and the influence of strong adsorbates may both play a role in catalyst deactivation as well. And the intrinsic activity of the catalyst is very likely positively related to secondary carbon oxidation. Different kinds of active sites are known to be present on the Pt surface, and the selectivity and deactivation speed of those could be vastly different. Further work combining kinetic experiment and surface characterization studies are required to test these ideas.

6. To test the generality of the structure sensitivity in mild reactions, the same series of catalysts could be used for other reaction systems such as the oxidation of other polyols, the oxidation of amines, the hydrogenation of polyunsaturated molecules, and others. Metals other than Pt, especially non-noble metals, shall also be tested. The study of each of these systems shall be carried out under strictly controlled conditions to exclude the effect of other factors.